# En route toward the peptide γ-helix: X-ray diffraction analyses and conformational energy calculations of Adm-rich, short peptides

**Daniela Mazzier,[a] Luigi Grassi,[a] Alessandro Moretto,[a,b] Carlos Alemán,[c] Fernando Formaggio,[a,b] Claudio Toniolo[a,b] and Marco Crisma[b]***

[a] *Department of Chemistry, University of Padova, 35131 Padova, Italy*

[b] *Institute of Biomolecular Chemistry, Padova Unit, CNR, 35131 Padova, Italy*

[c] *Departament d'Enginyeria Quimica, ETSEIB, Universitat Politècnica de Catalunya, 08028 Barcelona, Spain*

---

**Correspondence to:* Dr. Marco Crisma, Institute of Biomolecular Chemistry, Padova Unit, CNR, via Marzolo 1, 35131 Padova, Italy. E-mail: marco.crisma@unipd.it

(**Abstract)**

**We performed the solution-phase synthesis of a set of model peptides, including homo-oligomers, based on the 2-aminoadamantane-2-carboxylic acid (Adm) residue, an extremely bulky, highly lipophilic, tricyclic, achiral, $C^{\alpha}$-tetrasubstituted α-amino acid. In particular, for the difficult peptide coupling reaction between two Adm residues, we took advantage of the Meldal's α-azidoacyl chloride approach. Most of the synthesized Adm peptides were characterized by single-crystal X-ray diffraction analyses. The results indicate a significant propensity for the Adm residue to adopt γ-turn / γ-turn-like conformations. Interestingly, we found that a -CO-$(Adm)_2$-NH- sequence is folded in the crystal state into a regular, incipient γ-helix, at variance with the behavior of all of the homo-dipeptides from $C^{\alpha}$-tetrasubstituted α-amino acids already investigated, which tend to adopt either the β-turn or the fully-extended conformation. Our DFT conformational energy calculations on the terminally blocked homo-peptides (*n* = 2-8) fully confirmed the crystal-state data, strongly supporting the view that this rigid $C^{\alpha}$-tetrasubstituted α-amino acid residue is largely the most effective building block for γ-helix induction, although to a limited length (anti-cooperative effect).**

**Keywords:** Adm peptides; conformational energy calculations; γ-helix; X-ray diffraction; γ-turns

**Running title:** EN ROUTE TOWARD THE PEPTIDE γ-HELIX

## Introduction

Among the known four helices in a system of five-linked peptide units stabilized by consecutive intramolecularly C=O…H-N H-bonds [1-8] running in the common direction (*i.e.*, from a downstream N-H donor to an upstream C=O acceptor), the α- [2,3], $3_{10}$- [6,9,10] and π- [5] helices have been much more extensively investigated, both theoretically and experimentally, than the γ-helix [6,11]. This latter 3D-structure should not be mixed up with either: (i) the "γ-helix" or 5.1-helix proposed by Pauling 65 years ago [2,3] as an alternative possibility to its celebrated α-helix, but, although discussed by Prasad and Singh in 1981 [12], never found experimentally, or (ii) the "γ-helix" terminology proposed by Ramachandran [cited in ref. 13] to be used as a generic name for all polypeptide conformations strictly related to those of the three individual collagen helices.

A fully developed γ-helix, also termed $2.2_7$-helix [6], is generated by a set of at least three consecutive γ-turns [6,11,14-24]. It is characterized by 2.2 amino acid residues per turn, a rise per residue of 2.75 Å, and seven atoms in the *pseudo*-cyclic ($C_7$) structures closed by the C(1)=O(1) ← H(3)-N(3) intramolecular H-bond. When the side chain (R) of the single α-amino acid completely involved in this main-chain reversal motif is different from hydrogen, two stereoisomers can take place with their $C^{\alpha}$-substituent located either in the axial or in the equatorial position relative to the H-bonded seven-membered *pseudo*-cycle. For an α-amino acid of the L-configuration, the ϕ,ψ backbone torsion angles are approximately 75°, -65° (the less stable, "classical" γ-turn) or -75°, 65° (the more stable, "inverse" γ-turn), respectively. Therefore, a *regular* and *fully developed* γ-helix is expected to exhibit the same position (either all axial or all equatorial) for the side chains of at least three consecutive residues with the same configuration and with identical sets (either all +/- or all -/+) for the signs of their backbone torsion angles. However, in the case of a $C^{\alpha}$-tetrasubstituted α-amino acid, as the one discussed in this article (see below), the differentiation between classical and inverse γ-turns based on the spatial disposition of the single side chain of $C^{\alpha}$-trisubstituted α-amino acids is not applicable because of the occurrence of two $C^{\beta}$ atoms in the former residue. As a result, here the two types of γ-turn become one the mirror image of the other.

*No example of any of these two types of γ-helix* (Figure 1) *has been unambiguously authenticated experimentally to date, neither in synthetic peptides nor in proteins*. However, to this aim, only a few compounds have been investigated and a few attempts have been made. Two *incipient* γ-helices (with only two consecutive γ-turns) were established in proteins by X-ray diffraction and reported in the literature. In the complex between an enzyme (porcine pancreatic

elastase) and an inhibitor (elafin), a severely distorted γ-turn is immediately followed by an inverse γ-turn [25]. In the complex between an enzyme (histone-H3 demethylase) and a derivative of a shortened H3, *three* γ-turns were observed, but two initial classical γ-turns are followed by an inverse γ-turn [26]. Also, in a solution NMR study it was shown that a peptide segment from the MUC1 protein core exhibits two (or perhaps three) consecutive γ-turns in the conformational equilibrium mixture [27]. Interestingly, two consecutive, intramolecularly H-bonded γ-turns in a linear peptide, with identical sets (-/+) for the signs of their backbone torsion angles, were seen in the crystal state for a terminally blocked dipeptide [28]. However, as in the heterochiral sequence -L-Pro-D-$c_3$Dip- ($c_3$Dip, 2,2-diphenyl-1-aminocyclopropane-1-carboxylic acid, a $C^{\alpha}$-tetrasubstituted α-amino acid; Figure 2) of this *incipient* γ-helix the amino acid at position 1 lacks the H-bonding donor N-H function, multiple elongation of the same dipeptide might at best give rise to a *γ-turn ribbon spiral*, similar to one of the two possible structures proposed by Venkataram Prasad and Balaram [29] for the $(Aib\text{-}L\text{-}Pro)_n$ (Aib, α-aminoisobutyric acid) polypeptide sequence, not to a regular, fully H-bonded, γ-helix.

Among the variety of building blocks suggested as efficient γ-turn inducers or mimics [see, for example, refs. 11, 30-35] which might be useful for the construction of γ-helices, we selected the $C^{\alpha}$-tetrasubstituted, achiral 2-aminoadamantane-2-carboxylic acid (Adm; Figure 2) because: (i) its preparation from the commercially available 2-adamantone [36-40] and (ii) an initial solution investigation by NMR and IR absorption [35] on one derivative, Ac-Adm-NHMe (Ac, acetyl; NHMe, methylamino) and one very short peptide, the terminally blocked dipeptide Ac-Adm-Gly-NHMe, were already reported. In this latter publication, this α-amino acid was proposed as a "promising γ-turn inducer for synthetic peptides". We were also intrigued by the opportunity to expand the large conformational versatility of the class of $C^{\alpha}$-tetrasubstituted residues, already clearly demonstrated in our long-standing 3D-structural investigations, which goes from $3_{10}$- and α-helices [9,10] to the fully-extended conformation [41]. In the crystal state, only the 3D-structures of the free Adm amino acid itself [39,42] and a few derivatives [36,39,43-47] were reported. An NMR analysis of a terminally-free tetrapeptide containing an Adm residue at position 3 was published [48] but without any discussion on its preferred conformation.

An additional, important motivation to unveil the 3D-structural propensity of peptides based on an amino acid residue (Adm) characterized by the diamondoid [49-52] adamantane [53-55] hydrocarbon cage, is related to its known properties and applications [36,39,43-45,56-58] in

medicinal chemistry, specifically in the areas of amino acid transport inhibition and neurotensin receptor antagonism for use in cancer research.

## Results and Discussion

### Adm Derivative and Peptide Syntheses

Following the procedure reported by Baxendale *et al.* [36], we synthesized the free, rigid, highly lipophilic, tricyclic Adm α-amino acid hydrochloride [36-40] *via* a variant of the classical Strecker synthesis as the hydrolytic step of its last intermediate, 2-benzamidoadamantane-2-carboxylic acid, proceeds under relatively mild acidic conditions, affording the desired compound free from the impurities characteristic of the Bucherer-Bergs strategy. The last step of this latter reaction (basic hydrolysis of the hydantoin intermediate) requires very severe experimental conditions [37] resulting in the production of a significant amount of inorganic impurities. In our procedure, we identified the following synthetic intermediates, all of them described in the literature except the first: 2-hydroxyadamantane-2-carbonitrile (cyanohydrin), 2-aminoadamantane-2-carbonitrile [36,38,59], 2-benzamidoadamantane-2-carbonitrile [36,38], and 2-benzamidoadamantane-2-carboxylic acid [36,38,39]. In the 3D-structure of the crystalline Adm cyanohydrin, solved by X-ray crystallography, two independent molecules characterize the asymmetric unit (Figure 3). In the packing mode, the hydroxyl group of molecule **A** is H-bonded to the cyano group of molecule **B** within the same asymmetric unit, while the hydroxyl group of molecule **B** is H-bonded to the cyano group of a (-*x*, -*y*, ½+*z*) symmetry equivalent of molecule **A**. As a result, H-bonded **A** and **B** molecules alternate in a sort of meander motif which propagates along the *c* direction.

The preparations of a very limited number of Adm containing peptides (all of them as short as dipeptides) were reported in the literature [35,60]. Three sequences of the general type -Adm-Xxx- (where Xxx is Gly, L-Leu or L-Phe) were synthesized more than 40 years ago either *via* the Adm N-carboxyanhydride (NCA) or the N-acetyl / trifluoroacetyl (Tfa) Adm 5(4*H*)-oxazolone C-activation methods in moderate to good yields. However, removal of the Tfa protection required unusually drastic alkaline conditions owing to the steric bulk of the nearby Adm residue. Interestingly, in the reaction with the $N^{\alpha}$-unprotected Adm NCA the very poor reactivity of the

Adm α-amino function precluded further elongation of the dipeptides. However, two sequences of the general type -Xxx-Adm- (where Xxx is L-Leu or Gly) were prepared in good yields (77 and 89%, respectively), in both cases using the strong Pht (phthaloyl)-Xxx-Cl C-activated derivative in the peptide coupling step. Removal of the Pht $N^{\alpha}$-protection by use of the effective nucleophilic hydrazine reagent, however, afforded the $N^{\alpha}$-dephthaloylated dipeptides in only poor yields.

In our present *initial* (not optimized) synthetic effort, in search of promising Adm model compounds potentially suitable to generate the peptide γ-helix, we envisaged two distinct routes: (a) preparation of -Adm-Xxx- (Xxx = protein amino acid) dipeptides, where the Adm residue, located at the N-terminus, is $N^{\alpha}$-protected by an easily removable urethane-type moiety, obtained by a C-activation method of current use, *e.g.* with the N-ethyl-N′-[3-(dimethylamino)propyl] carbodiimide (EDC) and 7-aza-1-hydroxy-1,2,3-benzotriazole (HOAt) [61], and (b) preparation of the unknown *homo*-oligopeptides of general formula -$(Adm)_n$-. To date, we were able to synthesize and characterize chemically and crystallographically the following set of peptides: Z-Adm-Gly-OEt (Z, benzyloxycarbonyl; OEt, ethoxy) and Z-Adm-L-Ala-OMe (OMe, methoxy) following route (a); and "$N_3$"-$(Adm)_2$-NH*i*Pr (NH*i*Pr, isopropylamino), H-$(Adm)_2$-NH*i*Pr, Tfa-$(Adm)_2$-NH*i*Pr, and "$N_3$"-$(Adm)_3$-NH*i*Pr, in addition to the crystalline side product N,N′-*bis*-[$(Adm)_2$-NH*i*Pr]oxalamide isolated from the reaction between H-$(Adm)_2$-NH*i*Pr and the C-activating reagent oxalyl chloride [62-64] following route (b).

For the synthesis of the extremely sterically hindered Adm homo-peptides, we typically took advantage of the highly C-activated acyl chloride derivatives [62-65] in combination with the small-size azido (termed in this paper "$N_3$") α-amino group precursor, following the general procedure developed by Meldal and coworkers [66-68]. In our synthetic approach, the Adm α-azido acid was converted *in situ* into its acyl chloride derivative by use of the valuable reagent oxalyl chloride. The "$N_3$" group was modified to amine by Pt/C catalytic hydrogenation with a yield from good to moderate, decreasing with peptide lengthening. The promising yield (67%) obtained in the coupling reaction leading to the homo-dipeptide alkylamide unfortunately dropped to 9% in the case of its higher homolog. This latter poor outcome was the main reason which prevented us to appropriately modify by acylation or further elongate the Adm homo-tripeptide alkylamide chain to the level required for a potential crystallographic characterization of a fully developed peptide γ-helix (it is worth noting that the "$N_3$" group, at variance with any amino protecting group bearing the C=O functionality, such as Z or Tfa used in this work, does not behave as a H-bonding acceptor).

**Crystal-State Conformational Analysis**

The molecular structures of "$N_3$"-Adm-NH*i*Pr, Z-Adm-OH, Z-Adm-NH*i*Pr, N,N′-*bis*-[$(Adm)_2$-NH*i*Pr]oxalamide, Z-Adm-Gly-OEt, Z-Adm-L-Ala-OMe, H-$(Adm)_2$-NH*i*Pr, "$N_3$"-$(Adm)_2$-NH*i*Pr, Tfa-$(Adm)_2$-NH*i*Pr, and "$N_3$"-$(Adm)_3$-NH*i*Pr, as determined by single-crystal X-ray diffraction analyses, are illustrated in Figures 4-13, respectively. Backbone torsion angles are listed in Table 1. For the structures belonging to a centrosymmetric space group, *i.e*. containing molecules of both handedness in the crystal cell, the molecule with a negative value of the $\phi$ torsion angle was selected as the asymmetric unit. Intra- and intermolecular H-bond parameters are reported in Table 2.

Bond lengths and bond angles (deposited; see *Materials and Methods*) are in general agreement with previously reported values for the geometry of the benzyloxycarbonylamino [69] moiety, the amide [70,71], ester [72] and azide [73] groups, and the peptide unit [74,75].

In the 3D-structure of "$N_3$"-Adm-NH*i*Pr (Figure 4), the N1-C1A and C1-NT bonds are nearly perpendicular to each other, the value of the $\psi$ backbone torsion angle being -92.80(14)°. The C-terminal amide unit is in the usual *trans* disposition (Table 1). It is worth recalling that for Adm residues in which the amino functionality is replaced by an azide moiety, a backbone $\phi$ torsion angle cannot be defined. In any case, the values adopted by the torsion angles N01-N1-C1A-C1, N01-N1-C1A-C1B1, and N01-N1-C1A-C1B2 [64.01(16)°, -61.04(18)°, and -179.16(14)°, respectively] suggest that a staggered disposition of the azide group relative to the C′ and the two $C^{\beta}$ substituents might be instrumental in minimizing unfavorable intramolecular steric contacts. Indeed, such $g^+,g^-,t$ arrangement is also observed for "$N_3$"-$(Adm)_3$-NH*i*Pr, whereas a $g^-,t,g^+$, disposition of the azide moiety is found for "$N_3$"-$(Adm)_2$-NH*i*Pr. The packing mode is characterized by an intermolecular H-bond between the isopropylamide NT-HT group and a ($x$, $-y$, $z+1/2$) symmetry equivalent of the O1 atom (Table 2), which connects molecules along the *c* direction.

In the 3D-structure of Z-Adm-OH (Figure 5), the disposition of the Z-urethane group, described by the $\theta^1$ and $\omega_0$ torsion angles, is the usual *trans*, *trans* or type-*b* conformation [69], the values of the C07-OU-C0-N1 and OU-C0-N1-C1A torsion angles being -179.18(13)° and 179.96(12)°, respectively. The $\theta^2$ (C01-C07-OU-C0) torsion angle, which defines the disposition of the phenyl ring relative to the urethane moiety, is also *trans* [-168.7(13)°]. The Adm residue adopts a helical conformation, with $\phi,\psi$ = -57.44(15)°, -50.52(14)°. Two types of intermolecular H-bonds

characterize the packing mode, namely between the (urethane) N1-H1 group and a (-*x*+2, -*y*+1, -*z*) symmetry equivalent of the (carboxylic acid) OT atom, and between the (carboxylic acid) OT-HT group and a (-*x*+2, -*y*, -*z*) symmetry equivalent of the (urethane carbonyl) O0 atom, thus generating interconnected centrosymmetric dimers.

In the 3D-structure of Z-Adm-NH*i*Pr (Figure 6), the $\theta^1$ and $\omega_0$ torsion angles of the Z-urethane group are both *trans* [-175.55(14)° and 178.05(12)°, respectively], whereas the value of $\theta^2$ is 106.15(18)°. The C-terminal amide $\omega_1$ torsion angle, -170.58(14)°, does not deviate much from the *trans*-planarity. The conformation of the Adm residue is characterized by $\phi$ = -72.22(15)° and $\psi$ = 91.66(14)°. These values, although not far from those expected for a γ-turn, do not allow the formation of an intramolecular H-bond between the NT-HT group and the (urethane carbonyl) O0 atom of acceptable geometry. Indeed, as reported in Table 2, the NT…O0 distance, 3.045(17) Å would seem appropriate, but the H…O separation of 2.70 Å exceeds the commonly accepted limit of 2.50 Å for the occurrence of a H-bond, and the N-H…O angle, 105.3°, is much narrower than 120° [76-79]. On these bases, we classify the conformation adopted by Adm in this structure as "open γ-turn". The lack of the intramolecular H-bond that would stabilize the γ-turn might be related to the involvement of the NT-HT group in an intermolecular H-bond. Specifically, in the packing mode, the NT-HT group is intermolecularly H-bonded to a (-*x*+1, -*y*+1, -*z*) symmetry equivalent of the (urethane carbonyl) O0 atom (Table 2). An additional, intermolecular H-bond is observed between the (urethane) N1-H1 group and a (-*x*+1, -*y*, -*z*) centrosymmetric equivalent of the (amide) O1 atom.

N,N′-*bis*-[$(Adm)_2$-NH*i*Pr]oxalamide was obtained as a synthetic byproduct during the oxalyl chloride-mediated coupling of "$N_3$"-Adm-OH with H-$(Adm)_2$-NH*i*Pr. In its crystal structure (Figure 7) the corresponding backbone torsion angles in the two halves of the molecule are opposite in sign and have similar, but not identical, absolute values (Table 1). The difference is even larger at the level of the two terminal isopropyl groups, which are oriented in a way not amenable to a *pseudo*-centrosymmetric arrangement, the values of the C2-NTA-CT1A-CT2A and C2-NTA-CT1A-CT3A torsion angles being 113.4(8)° and -124.3(7)°, respectively, in one half of the molecule, whereas in the second half the values of the corresponding C4-NTB-CT1B-CT2B and C4-NTB-CT1B-CT3B torsion angles are 79.6(11)° and -60.1(11)°, respectively. The central oxalamide unit is *trans*-planar [N1-C0A-C0B-N3 torsion angle -179.6(6)°]. All amide and peptide bonds are *trans*, with deviations from the *trans*-planarity (180°) not exceeding ±7.7°. Both Adm residues proximal to the oxalamide linkage (numbered 1 and 3 in Figure 7 and Table 2) are folded in a γ-turn, stabilized by an

intramolecular hydrogen bond between the NH group of Adm(2) and the (oxalamide carbonyl) O0A atom in one half of the molecule, while between the NH group of Adm(4) and the (oxalamide carbonyl) O0B atom in the second half. Both H-bonds display more than acceptable geometrical parameters (Table 2). Torsion angles characterizing the two γ-turns are $\phi_1,\psi_1$ = -74.5(6)°,85.9(5)° and $\phi_3,\psi_3$ = 73.1(6)°,-80.4(5)°. The two C-terminal Adm residues [Adm(2) and Adm(4)] show torsion angles not dramatically dissimilar from those reported above for Adm(1) and Adm(3), respectively, except that the absolute values of the ψ torsion angles are significantly larger. Specifically, $\phi_2,\psi_2$ = -69.3(6)°,97.9(6)° and $\phi_4,\psi_4$ = 65.6(6)°,-100.8(6)°. As a result, the expected NTA-HTA…O1 and NTB-HTB…O3 intramolecular H-bonds do not occur (Table 2) and the conformations adopted by the two C-terminal Adm residues belong to the open γ-turn type. In the packing mode, the NTA-HTA and NTN-HTB groups are intermolecularly H-bonded, respectively to the (*x*, *y*+1, *z*) translational equivalent of the O3 atom and to the (*x*, *y*-1, *z*) translational equivalent of the O1 atom. The N2-H2 and N4-H4 groups, already intramolecularly engaged, do not participate in the intermolecular H-bonding scheme. Additional intermolecular H-bonds involve the OH groups of the two cocrystallized methanol molecules as the donors, and the O2 and O4 amide oxygen atoms as the acceptors (Table 2).

An open γ-turn at the level of the Adm residue is also observed in the 3D-structure of the terminally protected dipeptide Z-Adm-Gly-OEt (Figure 8 and Table 2), in which $\phi_1,\psi_1$ are -72.85(14)°, 98.50(12)°. The C-terminal Gly residue is *semi*-extended [$\phi_2,\psi_2$ = 77.93(17)°,-172.00(13)°. The conformation of the Z-urethane group is described by $\omega_0$ = 173.70(11)°, $\theta^1$ = -179.09(11)°, and $\theta^2$ = 103.03(14)°. As for the C-terminal ethyl ester group [72], the ester bond is *trans* [$\omega_2$ = 179.37(19)°], and the value of the C2-OT-CT1-CT2 torsion angle is 179.92(19)°. Also in this case, the N-H group belonging to the open γ-turn, namely N2-H2, is intermolecularly H-bonded, the acceptor being the (-*x*+1, -*y*+1, -*z*) centrosymmetric equivalent of the (urethane carbonyl) O0 atom. A second intermolecular H-bond connects the N1-H1 group to the (peptide) O1 atom (symmetry equivalence: -*x*+1, -*y*, -*z* ).

Two independent molecules (**A** and **B**) characterize the asymmetric unit of Z-Adm-L-Ala-OMe. In both molecules, the -Ala-OMe moiety is disordered and was refined on two sets of positions. The major conformers (70% occupancy) of the two molecules are illustrated in Figure 9. In the crystal they are arranged in a *pseudo*-centrosymmetric disposition (not shown) which is violated by the configuration of L-Ala, common to both molecules. The backbone torsion angles of molecule **A** are very close in absolute value but opposite in sign to those of molecule **B**.

Specifically, in molecule **A**, the Adm residue adopts an open γ-turn conformation with ϕ positive and ψ negative [$\phi_1,\psi_1$ = 69.4(7)°, -94.5(6)°] and L-Ala is left-handed helical [$\phi_2,\psi_2$ = 42.5(9)°, 48.8(19)°], whereas in molecule **B** the Adm residue adopts an open γ-turn conformation with ϕ negative and ψ positive [$\phi_1,\psi_1$ = -70.6(6)°, 93.9(6)°] and L-Ala is right-handed helical [$\phi_2,\psi_2$ = -45.0(10)°, -47.2(11)°]. In both molecules, the Z-urethane C=O and the Ala N-H groups are too far apart for the occurrence of an intramolecularly H-bonded $C_7$ form (Table 2). The minor conformer of the -L-Ala-OMe moiety of molecule **A** is also left-handed helical [$\phi_2,\psi_2$ = 66(2)°, 33(5)°] as its major counterpart, whereas the minor conformer of the -L-Ala-OMe moiety of molecule **B** is located in the "bridge" region [80] of the conformational map [$\phi_2,\psi_2$ = -92.4(8)°, 12.1(5)°]. Again, the N-H groups belonging to an open γ-turn are intermolecularly H-bonded in the crystal packing. Specifically, the N2-H2 group of molecule **A** is H-bonded to the (*x*+1, y, *z*) translational equivalent of the (urethane carbonyl) O0B of molecule **B**, and the N4-H4 group of molecule **B** is H-bonded to the (*x*-1, y, *z*) translational equivalent of the (urethane carbonyl) O0A of molecule **A** (Table 2). Additional H-bonds are observed between the two independent molecules within the same asymmetric unit, namely from the N1-H1 group (molecule **A**) to the O3 atom (molecule **B**) and from the N3-H3 group (molecule **B**) to the O1 atom (molecule **A**). As a result, rows of alternating **A**-**B**-**A**-**B** molecules, each linked to the next by two H-bonds, are generated along the *a* direction

The conformation of the molecule arbitrarily chosen as the asymmetric unit in the centrosymmetric structure of H-$(Adm)_2$-NH*i*Pr (Figure 10) is described by the following values for the backbone torsion angles: $\psi_1$ = -71.4(3)°; $\phi_2,\psi_2$ = -80.5(4)°, 96.1(3)°. The values of the ϕ,ψ torsion angles adopted by the C-terminal residue, although not far from those expected for a γ-turn, do not allow the formation of the related ($C_7$) intramolecular H-bond. Indeed, the NT…O1 and HT…O1 separations are 3.293(4) Å and 2.97 Å, respectively, and the NT-HT…O1 angle is 105°. In the packing mode, both the (amino) N1-H1A and the (peptide) N2-H2 groups are intermolecularly H-bonded to the (amide carbonyl) O2 atom of a (-*x*, -*y*, -*z*) symmetry related molecule (Table 2), thus generating a centrosymmetric dimer. In addition, the (amide) NT-HT group is H-bonded to the (1-*x*, -*y*, -*z*) symmetry equivalent of the (peptide) O1 atom, connecting molecules along the *a* direction. The second H-atom of the N-terminal amino group, H1B, is not involved in any H-bond.

The 3D-structure of "$N_3$"-$(Adm)_2$-NH*i*Pr is illustrated in Figure 11. The backbone conformation closely mirrors that of H-$(Adm)_2$-NH*i*Pr described above. Indeed, the values of $\phi_2,\psi_2$ differ by less than 1.2° in the two compounds (Table 1), thus resulting in the same open γ-turn conformation. The $\psi_1$ torsion angle is negative in both structures, and slightly larger for "$N_3$"-

$(Adm)_2$-NH*i*Pr [-81.6(2)°] than for H-$(Adm)_2$-NH*i*Pr [-71.4(3)°]. The only other significant difference, in terms of molecular conformation, between the two structures is found at the level of the C-terminal amide group, almost perfectly *trans*-planar in "$N_3$"-$(Adm)_2$-NH*i*Pr [$\omega_2$ = 179.5(5)°], while slightly distorted in H-$(Adm)_2$-NH*i*Pr [$\omega_2$ = -169.9(3)°]. In the packing mode of "$N_3$"-$(Adm)_2$-NH*i*Pr, the N2-H2 and NT-HT groups are intermolecularly H bonded, respectively, to the (-*x*+2, -*y*+1, -*z*) centrosymmetric equivalent of the (amide carbonyl) O2 atom and to the (-*x*+2, -*y*, -*z*) symmetry equivalent of the (peptide) O1 atom (Table 2).

In the 3D-structure of Tfa-$(Adm)_2$-NH*i*Pr (Figure 12), the N-terminal Adm is folded in a γ-turn conformation stabilized by an intramolecular H-bond between the (peptide) N2-H2 and the (trifluoroacetamido) C0=O0 groups. The H…O separation, 2.54 Å, only marginally exceeds the commonly accepted upper limit of 2.50 Å for the occurrence of a H-bond, while the N-H…O angle, 123°, is larger than 120° [76-79]. The observation that the N2-H2 and C0=O0 groups are not involved in any *inter*molecular H-bond supports the view that the N2-H2…O0 intramolecular interaction reported above is a true H-bond. The values of the ϕ,ψ torsion angles of the Adm(1) residue involved in the γ-turn are -78.7(3)° and 88.1(2)°. Conversely, the C-terminal Adm(2) residue, with $\phi_2,\psi_2$ = -60.8(3)°, -65.5(2)° is helical. This structure offers a case study to unravel intramolecular features which may be different when an Adm residue is accomodated in the γ-turn or in a helical conformation. A number of C-H…H-N and C-H…O intramolecular contacts shorter than the sum of their van der Waals radii (H…H 2.40 Å, H…O 2.72 Å) are found for both Adm(1) and Adm(2) residues. Interestingly, the carbonyl oxygen of the Adm(1) residue involved in the γ-turn sits quite comfortably right in between the H atoms of the (*pro-S*)-$C^{\beta}$ and of one of the $C^{\gamma}$ atoms of the same residue, with H…O distances of 2.58 Å and 2.60 Å, respectively. Conversely, as a result of the different sign and value for the ψ torsion angle, the carbonyl oxygen of the helical Adm(2) residue is located at 2.64 Å from the (*pro-R*) β-CH, but much closer, 2.36 Å to one of the γ-CH atoms. The intra-residue distances between the carbonyl oxygen and the side-chain β- and γ-CH groups are governed by the ψ torsion angle. It appears that the ψ value of Adm(1), 88.1(2)°, is associated to much less unfavorable short contacts than that of Adm(2), -65.5(2)°. Indeed, model building suggests that ψ values typical for regular, right-handed helices (-30° ÷ -45°) are strongly disallowed for Adm, as they would bring one of the γ-CH atoms at 2.10 ÷ 2.15 Å from the carbonyl oxygen. In the packing mode of Tfa-$(Adm)_2$-NH*i*Pr, the N1-H1 group is H-bonded to a (-*x*, -*y*, -*z*+1) symmetry equivalent of the (peptide) O1 atom, thus generating a centrosymmetric dimer. As for the remaining, potential H-bonding donor, the (isopropylamide) NT-HT group, the only acceptor within

reach is a (-*x*+1/2, *y*-1/2, -*z*+3/2) symmetry equivalent of the O2 atom, although the N…O and H…O distances are significantly long (Table 2). This latter, weak intermolecular H-bond connects molecules in a zig-zag motif along the *b* direction.

Finally, the crystal state conformation of "$N_3$"-$(Adm)_3$-NH*i*Pr (Figure 13) is characterized by two, consecutive γ-turns at the level of the Adm(2) and Adm(3) residues. The N3-H3…O1 and NT-HT…O2 intramolecular H-bonds display more than acceptable geometries (Table 2), with H...O distances in the range 2.27 ÷ 2.44 Å and a value of 132° for both N-H…O angles. The sets of backbone torsion angles for the residues involved in the two γ-turns are $\phi_2,\psi_2$ = -81.91(18)°, 84.20(16)° and $\phi_3,\psi_3$ = -72.98(19)°, 75.88(18)°. As both γ-turns share the same set of signs (*i.e.*, -/+) for the backbone torsion angles, they give rise to an *incipient γ-helix*. The ψ value of the N-terminal "$N_3$"-Adm residue is 77.87(17)°. All of the ω torsion angles deviate less than ±9° from the ideal *trans*-planarity (Table 1). Notably, the packing mode is not stabilized by any N-H…O intermolecular H-bond. Indeed, the only potential H-bonding donor not already intramolecularly engaged is the N2-H2 group, which is deeply buried between the proximal, bulky adamantane cages. Conversely, in addition to intermolecular van der Waals interactions, a few C-H…O or C-H…N short contacts with H…O(N) distances in the range 2.69 ÷ 2.79 Å and C-H…O(N) angles within 144 ÷ 172° are observed, namely between the CT3 methyl group and a (*x*+1, *y*, *z*) symmetry equivalent of O3, between the C1G1 methylene of Adm(1) and a (-*x*+1, -*y*+2, -*z*+1) symmetry equivalent of the (azido) N02 atom, and between the C1G3 methylene of Adm(1) and a (-*x*+2, -*y*+2, -*z*+1) symmetry equivalent of the (azido) N1 atom.

Overall, in the 3D-structures described above, none of the N-H groups involved in a γ-turn characterized by an acceptable intramolecular H-bond geometry turns out to take part in the intermolecular H-bonding network. Conversely, for all of the cases which we classify as open γ-turns, the N-H group potential donor for the occurrence of the intramolecularly H-bonded $C_7$ form is always intermolecularly engaged.

In this work, the backbone conformations of fifteen examples of N-acylated Adm residues (*i.e.*, not taking into account those in which the amino group at the N-terminus is free or replaced by an azido group) have been determined. The resulting ϕ,ψ scatterplot, normalized to the negative sign for the ϕ torsion angle, is illustrated in Figure 14 (left).

We found only two examples of helical Adm residues (black triangles in Figure 14), including Z-Adm-OH which carries a free carboxylic acid group (at variance with all other Adm residues reported in Figure 14 which are followed by an amide or peptide bond). The ϕ values are in

the range -57° ÷ -61°, a common observation for helical $C^{\alpha}$-tetrasubstituted α-amino acid residues [10], whereas the ψ values, from -51° to -66°, are larger in magnitude than those typical for $3_{10}$-helices (-30°) or α-helices (-42°) [9,81]. These findings compare well with the few occurrences of N-acylated Adm derivatives of the R-CO-Adm-OH or R-CO-Adm-OR′ type reported in the literature [36,39,43-47], from which the average values of ϕ,ψ = -54°, -55° can be calculated for a helical Adm residue.

Our remaining thirteen examples of Adm residues, characterized by opposite signs for the ϕ and ψ torsion angles, broadly belong to the γ-turn region in the upper left quadrant of the Ramachandran map, an expanded view of which is shown in Figure 14 (right). Here, we differentiate between γ-turns (red triangles), for which a C=O…H-N intramolecular H-bond of the $C_7$ type of "normal" geometry is observed (*i.e.*, H…O distance < 2.55 Å, and N-H…O angle > 120°; five examples), and open γ-turns (blue triangles), in which the H…O distance of the expected H-bond exceeds 2.55 Å (eight examples). In the five examples of γ-turns the ϕ values range from -73° to -82° and the ψ values from 76° to 88°. In the eight examples of open γ-turns the ϕ values range from -66° to -81° and the ψ values from 92° to 101°. The average backbone torsion angles are ϕ,ψ = -76°, 83° for regular, H-bonded γ-turns, while ϕ,ψ = -73°, 96° for the open γ-turns. These findings indicate that the key parameter determining the occurrence or the absence of the intramolecular H-bond of the $C_7$ type is the value of the ψ torsion angle, larger (> 90°) for the open γ-turns. Indeed, the value of ψ governs the orientation of the (*i*+1) N-H group. The observation that in all of our examples of open γ-turns the N-H group potential donor for the occurrence of the intramolecularly H-bonded $C_7$ form is involved in an intermolecular H-bond suggests that such opening of the γ-turns could be at least in part related to crystal packing effects. However, from the set of structures reported here, combined with those of Adm acylated derivatives described in the literature [36,39,43-47], it appears that Adm tends in general to adopt ψ values larger than those common for $C^{\alpha}$-tetrasubstituted α-amino acid residues, in all probability as a consequence of the severe steric hindrance of the bulky adamantane moiety.

It is worth comparing the values of ϕ,ψ = -76°, 83°, averaged from the five examples of H-bonded γ-turns found in this work, with those commonly considered typical for standard, inverse γ-turns, ϕ,ψ = -75°, 65°. While the values of ϕ agree well, our average ψ value is significantly larger. Also, from their computational investigation [14], Némethy and Printz inferred that some rotation (Δω) out of the *trans*-planarity of the peptide (amide) bonds is required for the formation of the

intramolecular H-bond in the γ-turn. Conversely, from our results, we observe that in four out of five γ-turns the amide bond following the Adm residue in the γ-turn is perfectly *trans*-planar (ω = 180°) within ±1°. The only exception is represented by the peptide bond between residues 2 and 3 in the structure of "$N_3$"-$(Adm)_3$-NH*i*Pr, for which Δω = 6.4°. Interestingly, this latter peptide bond is also preceding the second, consecutive γ-turn at the level of Adm(3). Values of |Δω| ranging from 4.0° to 8.8°, but not all of the same sign, characterize the amide bonds preceding the four remaining γ-turns.

From the analysis of the structures investigated in this work, an intriguing relationship emerged between the values of the bond angles at the quaternary α-carbon of Adm and the type of backbone conformation adopted. The results reported in Table 3 are normalized to the negative sign of the ϕ torsion angle. Specifically: (i) The N-$C^{\alpha}$-C′ (τ) bond angle is significantly compressed if compared to the standard tetrahedral value of 109.5°. The value of τ averaged from the Adm residues adopting a γ-turn / open γ-turn conformation, 104.5°, is 2.4° smaller than that observed for helical Adm residues (106.9°). Values of τ comparable to that of Adm in the γ-turn / open γ-turn conformation (or even lower) were documented for $C^{\alpha}$-tetrasubstituted α-amino acid residues adopting the fully-extended conformation [41]. (ii) The bond angle involving the two β-carbon atoms, internal to the Adm cage, is 108.2° for helical Adm residues, and 0.6° smaller for the γ-turn / open γ-turn conformation. (iii) The two β-carbon atoms are arranged asymmetrically with respect to the nitrogen atom. Specifically, the N-$C^{\alpha}$-$C^{\beta}$ bond angle involving the (*pro-S*)-$C^{\beta}$ ($C^{\beta 1}$ in Table 3) is smaller than tetrahedral, and that involving the (*pro-R*)-$C^{\beta}$ ($C^{\beta 2}$ in Table 3) is larger, when the sign of the ϕ torsion angle is negative. In the molecules where Adm adopts a left-handed screw sense (*i.e.*, ϕ positive), the reverse is true. The difference between the values of these two bond angles is 5.3° both for the helical and the γ-turn / open γ-turn conformations, although the values of the N-$C^{\alpha}$-$C^{\beta 1}$ and N-$C^{\alpha}$-$C^{\beta 2}$ bond angles are slightly different in the two conformations (N-$C^{\alpha}$-$C^{\beta 1}$ 106.9° *versus* 107.4°, respectively; N-$C^{\alpha}$-$C^{\beta 2}$ 112.2° *versus* 112.7°, respectively). (iv) On the carbonyl side, the C′-$C^{\alpha}$-$C^{\beta 1}$ and C′-$C^{\alpha}$-$C^{\beta 2}$ bond angles are equal (111.4°) when Adm is helical. Conversely, for Adm in the γ-turn / open γ-turn conformation with a positive sign of the ψ torsion angles, the value of the C′-$C^{\alpha}$-$C^{\beta 2}$ bond angle (114.8°) is much larger than that involving the $C^{\beta 1}$ atom (109.6°). The difference between these two latter values, 5.2°, is much larger than any difference between corresponding bond angles at the α-carbon of Aib, for which a conformation and screw-sense dependent asymmetry is well documented [10,82].

**Conformational Energy Calculations**

The cooperative or anti-cooperative energy associated to the generation of a consecutive γ-turn conformation (γ-helix) in Adm homo-peptides was determined by calculating the CE parameter (Eq 3 in *Materials and Methods*) for Ac-$(Adm)_n$-NHMe with *n* ranging from to 2 to 8 arranged in an all-γ-turn conformation. In these *n* homo-peptides, all residues were initially disposed in a γ-turn conformation, which was preserved after geometry optimization in all cases. According to the criteria defined in Eqs 1-3, CE is negative or positive in the presence of cooperative or anti-cooperative effects, respectively. It should be noted that CE represents a valuable parameter, which was already used to study the intrinsic tendency of both coded and non-coded amino acid residues to adopt regular conformations [83-85]. Our results, displayed in Figure 15, reveal unfavorable CE values, independently of *n*. Moreover, CE grows linearly with the number of Adm residues. These results indicate that the γ-turn conformation generates accumulative internal strains, which eventually result in anti-cooperative energy effects. Overall, these findings clearly suggest that the stability of the consecutive γ-turn conformation is expected to decrease with increasing length of the homo-peptide. This situation is opposite to that typically found in peptide secondary structures with cooperative inter-residue H-bonds between unstrained residues (*e.g.*, α-helix in Ala and Glu homo-peptides), in which a stabilizing effect with negative CE values is obtained [83-85].

Moreover, a comparison was performed among complete geometry optimizations, using as starting point conformations those with a β-turn [18,19,86] or two consecutive γ-turns, of Ac-$(Adm)_2$-NHMe, Ac-$(c_3Dip)_2$-NHMe, and Ac-$(Ac_6c)_2$-NHMe ($Ac_6c$, 1-aminocyclohexane-1-carboxylic acid) sequences. As Adm, both $c_3$Dip and $Ac_6c$ are $C^{\alpha}$-tetrasubstituted α-amino acids. The former was studied because it represents the driving force for double γ-turn formation in the dipeptide published by Cativiela and coworkers [28], while $Ac_6c$ bears the six-membered annular system typical of the tricyclic Adm residue. Our results, displayed in Table 4, indicate that for Ac-$(Adm)_2$-NHMe the free energy (ΔG) for the regular type-III β-turn conformation is unfavorable by 4.5 kcal/mol if compared to that of the two consecutive γ-turns, whereas this energy penalty is more than suppressed for Ac-$(c_3Dip)_2$-NHMe. These data strongly support the view that the Adm chemical structure is remarkably more suitable to stabilize consecutive γ-turns than that of $c_3$Dip [28]. More specifically, inter-residue interactions are very much repulsive for the regular type-III β-

turn of Ac-$(Adm)_2$-NHMe, in which the two adamantyl side cages face each other in close contact (Figure 16**C**). Conversely, the distance between the adamantyl groups increases considerably in the case of the two consecutive γ-turns (Figure 16**A**), resulting in a significant stabilization with respect to the regular β-turn. Moreover, the repulsive adamantyl···adamantyl interactions found for the regular type-III β-turn can be partially alleviated by considering a highly distorted type-II β-turn (Figure 16**B**), which nevertheless does preserve the characteristic *i*, *i*+3 intramolecular H-bonded ring of β-turns. In the type-II β-turn conformation the orientation of the central peptide bond is reversed if compared to those of type-I / type-III β-turns [86], thereby increasing the distance between the two Adm side groups and reducing their repulsive interactions. Consequently, the distorted type-II β-turn is 1.9 kcal/mol more stable than the regular type-III β-turn, although still 2.6 kcal/mol less stable than the conformation with two consecutive γ-turns. Overall, our results indicate that the factors governing the conformational preferences of Ac-$(Adm)_2$-NHMe are different from those of Ac-$(c_3Dip)_2$-NHMe. Indeed, the preferred conformation of the $c_3$Dip homo-dipeptide is induced not only by the onset of steric interactions between the two spatially close phenyl rings but particularly by the intriguing characteristics of the cyclopropane ring, which plays a crucial role owing to its intrinsic angular strain [87,88]. Finally, as for Ac-$(Ac_6c)_2$-NHMe, the regular (type-I) β-turn is favored by 0.4 kcal/mol with respect to the conformation with two consecutive γ-turns. This opposite trend was far from unexpected since the $Ac_6$c cyclohexane moiety is monocyclic (not tricyclic fused as in Adm) and its size is large enough to avoid any internal geometric strain (as in $c_3$Dip).

## Conclusions

A regular γ-helix (produced by a repetition of at least *three* consecutive, intramolecularly H-bonded, γ-turns of the same type) still remains to be discovered in synthetic peptides and proteins. In the present experimental work we clearly showed by X-ray diffraction on a variety of Adm derivatives and Adm-rich peptides, including homo-peptides, that this residue is endowed with a significant propensity to adopt γ-turn / γ-turn-like conformations. Moreover, the onset of an *incipient* γ-helix (with *two* consecutive γ-turns) was assessed in the synthetic, terminally blocked homo-dipeptide amide sequence -CO-$(Adm)_2$-NH-. Our conformational energy calculations on a large set of Adm

homo-oligomers strongly support the results arising from crystallography, specifically highlighting the unique property of this highly bulky $C^{\alpha}$-tetrasubstituted $\alpha$-amino acid residue in promoting this unprecedented peptide folded 3D-structure. We are confident that, when the current drawbacks in the synthesis of Adm long peptides will be overcome, this highly crystalline homo-oligomeric series will provide structural biochemists with the first experimental proof for the existence of this still missing peptide helix.

## Materials and Methods

### Synthesis and Characterization of the Novel Adm Derivatives and Peptides

Melting points were determined using a Leitz (Wetzlar, Germany) model Laborlux 12 apparatus and are not corrected. The mass spectra were recorded using a Mariner ESI-TOF (Perseptive Biosystem, Foster City, CA) mass spectrometer. The solid-state IR absorption spectra (KBr disk) were obtained with a Perkin-Elmer (Norwalk, CT) model 1720X FT-IR spectrophotometer. The $^{1}H$ and $^{13}C$ NMR spectra were recorded with a Bruker (Karlsruhe, Germany) model AC 200 spectrometer. Measurements were carried out in deuterated dimethylsulfoxide (DMSO-$d_6$) or deuterochloroform (99.96% *d*) (Aldrich, Milwaukee, WI, USA) with tetramethylsilane as the internal standard. Typical workup of the reaction mixtures and purification of the products included, as appropriate, washing of the organic solutions with aqueous $KHSO_4$ and $NaHCO_3$ (10% and 5%, respectively) and brine, and/or flash chromatography by use of a Merck silica gel 60 (40-63 μm mesh) stationary phase and $CH_2Cl_2$ / ethyl acetate or $CH_2Cl_2$ / MeOH solvent mixtures as eluants. All of the compounds were obtained in a chromatographically homogeneous state.

*2-Hydroxyadamantane-2-carbonitrile (cyanohydrin)* was prepared from 2-adamantone and KCN in a $CH_2Cl_2$ / acidic water mixture at room temperature under stirring. Yield: 95%. M.p. ???? °C 198-200°C. IR (KBr): 3401, 2239, 1698 $cm^{-1}$. $^{1}H$ NMR (DMSO-$d_6$, 200 MHz): δ 6.53, 2.07, 2.01, 1.87, 1.67, 1.54, 1.48 ppm. $^{13}C$ NMR (DMSO-$d_6$, 50 MHz): δ 123.08, 72.44, 36.60, 36.07, 34.31, 30.23, 25.90, 25.79 ppm. MS (ESI-TOF) [*m*/*z*]: $[M]_{calc}$ 177.12, $[M+H]^{+}_{exp}$ 178.15. Its chemical structure was further characterized by X-ray diffraction.

*"$N_3$"-Adm-OH* was prepared from HCl · H-Adm-OH and imidazol-1-sulfonylazide hydrochloride in MeOH in the presence of $CuSO_4 \cdot 5\ H_2O$ and $K_2CO_3$ at room temperature under stirring according to ref. [89]. Yield: 90%. M.p. ???? °C. IR (KBr): 2102, 1711, 1360 $cm^{-1}$. $^{1}H$ NMR ($CDCl_3$, 200 MHz): δ 2.29, 2.11-2.10, 1.84, 1.72, 1.65 ppm. $^{13}C$ NMR ($CDCl_3$, 50 MHz): δ 175.69, 57.15, 37.16, 34.76, 32.72, 31.86, 26.49 ppm. MS (ESI-TOF) [*m*/*z*]: $[M]_{calc}$ 221.12, $[M+H]^{+}_{exp}$ 222.14.

*"$N_3$"-Adm-NHiPr* was prepared from "$N_3$"-Adm-OH and isopropylamine in anhydrous $CH_2Cl_2$ in an inert atmosphere in the presence of EDC and HOAt first at 0°C, then at room temperature for 24 h under stirring, according to ref. [61]. Yield: 72%. M.p. ???? °C. IR (KBr): 3308, 2097, 1634, 1538, 1238 $cm^{-1}$. $^{1}H$ NMR ($CDCl_3$, 200 MHz): δ 5.54, 4.28-4.03, 2.20-2.06, 1.83-1.64, 1.19 ppm. $^{13}C$ NMR ($CDCl_3$, 50 MHz): δ 174.97, 57.11, 41.80, 37.24, 34.80, 33.01,

32.51, 26.54, 22.84 ppm. MS (ESI-TOF) [*m*/*z*]: $[M]_{calc}$ 262.19, $[M+H]^+_{exp}$ 263.19. Its chemical structure was further characterized by X-ray diffraction.

*H-Adm-NHiPr* was prepared by hydrogenation of "$N_3$"-Adm-NH*i*Pr in the presence of the Pd/C catalyst in MeOH at room temperature under stirring. Yield: 95%. M.p. ???? °C. IR (KBr): ????????????? $cm^{-1}$. $^1H$ NMR ($CDCl_3$, 200 MHz): δ 6.19, 4.18-4.01, 3.55, 2.16, 2.00-1.64, 1.17 ppm. $^{13}C$ NMR ($CDCl_3$, 50 MHz): δ 173.33, 62.21, 41.56, 37.84, 34.86, 34.40, 32.33, 26.88, 26.70, 22.63, 22.50 ppm. MS (ESI-TOF) [*m*/*z*]: $[M]_{calc}$ 236.19, $[M+H]^+_{exp}$ 237.20.

*Z-Adm-OH* was prepared from HCl · H-Adm-OH and Z-OSu [90,91] in $H_2O$ / 1,4-dioxane mixture in the presence of an excess of trimethylamine at 0°C under stirring. Yield: 35%. M.p. 107-109°C. IR (KBr): 3389, 3367, 2910, 1749, 1685 $cm^{-1}$. $^1H$ NMR ($CDCl_3$, 200 MHz): δ 7.35, 5.11, 5.06, 2.50, 1.76, 1.67, 1.54 ppm. MS (ESI-TOF) [*m*/*z*]: $[M]_{calc}$ 329.16, $[M+H]^+_{exp}$ 330.15. Its chemical structure was further characterized by X-ray diffraction.

*Z-Adm-NHiPr* was prepared from Z-Adm-OH and isopropylamine in anhydrous $CH_2Cl_2$ in the presence of EDC and HOAt at 0°C under stirring. Yield: 85%. M.p. . ???? °C. IR (KBr): 3364, 1716, 1615, 1529 $cm^{-1}$. $^1H$ NMR ($CDCl_3$, 200 MHz): δ 7.35, 6.73, 5.11, 4.81, 4.08, 2.62, 1.86, 1.77, 1.64, 1.13 ppm. MS (ESI-TOF) [*m*/*z*]: $[M]_{calc}$ 370.23, $[M+H]^+_{exp}$ 371.21. Its chemical structure was further characterized by X-ray diffraction.

*Z-Adm-Gly-OEt* was prepared from Z-Adm-OH and HCl · H-Gly-OEt in anhydrous $CH_2Cl_2$ in the presence of diisopropylethylamine, EDC, and HOAt at 0°C under stirring. Yield: 72%. M.p. . 123-125°C. IR (KBr): 3356, 1764, 1707, 1647, 1529 $cm^{-1}$. $^1H$ NMR ($CDCl_3$, 200 MHz): δ 7.35, 5.00, 4.80, 4.14, 3.95, 2.00, 1.76, 1.67, 1.54, 1.03 ppm. MS (ESI-TOF) [*m*/*z*]: $[M]_{calc}$ 414.22, $[M+H]^+_{exp}$ 415.21. Its chemical structure was further characterized by X-ray diffraction.

*Z-Adm-L-Ala-OMe* was prepared from Z-Adm-OH and HCl · H-L-Ala-OMe in anhydrous $CH_2Cl_2$ in the presence of diisopropylethylamine, EDC, and HOAt at 0°C under stirring. Yield: 61%. M.p. . 120-122°C. IR (KBr): 3361, 1750, 1700, 1642, 1534 $cm^{-1}$. $^1H$ NMR ($CDCl_3$, 200 MHz): δ 7.35, 4.93, 4.75, 4.60, 3.80, 2.20, 1.96, 1.87, 1.64, 1.47 ppm. MS (ESI-TOF) [*m*/*z*]: $[M]_{calc}$ 414.22, $[M+H]^+_{exp}$ 415.23. Its chemical structure was further characterized by X-ray diffraction.

*"$N_3$"-(Adm)$_2$-NHiPr* was prepared from "$N_3$"-Adm-OH and H-Adm-NH*i*Pr in anhydrous $CH_2Cl_2$ in an inert atmosphere in the presence of oxalyl chloride and diisopropylethylamine first at 0°C, then at room temperature for 24 h under stirring. Yield: 67%. M.p. ????°C. IR (KBr): 3391, 3318, 2089, 1655, 1643, 1523 $cm^{-1}$. $^1H$ NMR ($CDCl_3$, 200 MHz): δ 7.03, 5.57, 4.13-3.96, 2.72, 2.27-1.50, 1.20 ppm. $^{13}C$ NMR ($CDCl_3$, 50 MHz): δ 170.78, 170.65, 71.06, 64.72, 41.40, 37.43, 37.05, 34.58, 34.16, 32.97, 32.36, 32.30, 32.27, 26.74, 26.48, 26.39, 22.59 ppm. MS (ESI-TOF)

[*m*/*z*]: $[M]_{calc}$ 439.30, $[M+H]^+_{exp}$ 440.32. Its chemical structure was further characterized by X-ray diffraction.

*H-(Adm)$_2$-NHiPr* was prepared by hydrogenation of "$N_3$"-(Adm)$_2$-NH*i*Pr in the presence of the Pd/C catalyst in an EtOH / $CH_2Cl_2$ mixture at room temperature under stirring for 3 days. Yield: 30%. M.p. ????°C. IR (KBr): 3376, 3350, 1654, 1631, 1542, 1525 $cm^{-1}$. $^1H$ NMR ($CDCl_3$, 200 MHz): δ 7.02, 5.57, 4.14-3.97, 2.72, 1.91, 1.15 ppm. MS (ESI-TOF) [*m*/*z*]: $[M]_{calc}$ 413.31, $[M+H]^+_{exp}$ 414.33. Its chemical structure was further characterized by X-ray diffraction.

*Tfa-(Adm)$_2$-NHiPr* was prepared by heating at 50°C trifluoroacetic anhydride with H-(Adm)$_2$-NH*i*Pr in anhydrous $CHCl_3$ [37]. Yield: ??. M.p. ????°C. IR (KBr): ???????????? $cm^{-1}$. $^1H$ NMR ($CDCl_3$, 200 MHz): δ ?????????? ppm. MS (ESI-TOF) [*m*/*z*]: $[M]_{calc}$ 509.29, $[M+H]^+_{exp}$ 510.30. Its chemical structure was characterized by X-ray diffraction.

*"N$_3$"-(Adm)$_3$-NHiPr* was prepared from "$N_3$"-Adm-OH and H-(Adm)$_2$-NH*i*Pr in anhydrous $CH_2Cl_2$ in an inert atmosphere in the presence of oxalyl chloride and diisopropylethylamine first at 0°C, then at room temperature for 48 h under stirring. Yield: 9%. M.p. ????°C. IR (KBr): ???????????? $cm^{-1}$. $^1H$ NMR ($CDCl_3$, 200 MHz): δ 7.11, 6.94, 5.58, 3.98, 2.69, 1.89, 1.10 ppm. MS (ESI-TOF) [*m*/*z*]: $[M]_{calc}$ 616.41, $[M+H]^+_{exp}$ 617.44. Its chemical structure was further characterized by X-ray diffraction.

*N,N'-bis[(Adm)$_2$-NHiPr]-oxalamide* was obtained in an extremely limited amount as a crystalline side product in the synthesis of "$N_3$"-(Adm)$_3$-NH*i*Pr upon reaction of H-(Adm)$_2$-NH*i*Pr with oxalyl chloride [62-64]. Its chemical structure was characterized by X-ray diffraction.

**X-Ray Diffraction**

X-Ray diffraction data were collected with a Gemini E four-circle kappa diffractometer (Agilent Technologies) equipped with a 92-mm EOS CCD detector. Graphite monochromated Cu Kα radiation (λ = 1.54178 Å) was used for all structures except for 2-hydroxy-adamantane-2-carbonitrile, for which Mo Kα radiation (λ = 0.71069 Å) was exploited. Data collection and reduction were performed with the CrysAlisPro software (Agilent Technologies). A semi-empirical absorption correction based on the multi-scan technique using spherical harmonics, implemented in the SCALE3 ABSPACK scaling algorithm, was applied. The structures were solved by *ab initio* procedures of the SIR 2002 [92] or SIR 2014 [93] programs, and refined by full-matrix least-squares procedures on $F^2$, using all data, by application of the SHELXL-97 [94] or SHELXL-2014 [95] programs, with anisotropic displacement parameters for all of the non-H atoms. In general, H-atoms were calculated at idealized positions and refined using a riding model. Details of structure

solution and refinement specific to individual structures are given below. Relevant crystal data and structure refinement parameters are reported in the *Supporting Information* (Tables S1-S11). CCDC 1503357-1503367 contain the supplementary crystallographic data for this paper. The data can be obtained free of charge from The Cambridge Crystallographic Data Centre via www.ccdc.cam.ac.uk/structures.

*2-Hydroxy-adamantane-2-carbonitrile (cyanohydrin)*: The asymmetric unit is composed of two independent molecules (**A** and **B**). Interestingly, this achiral compound crystallizes in the chiral space group $Pna2_1$. Not unexpectedly, considering the lack of strong anomalous scatterers, the value of the Flack parameter was inconclusive [either 0.8(10) or 0.2(10) for the reported and the inverted structures, respectively]. On this basis, Friedel pairs were merged and no claim that the arbitrarily chosen enantiomorph corresponds to the absolute structure is made. The positions of the H-atoms of the hydroxyl groups were recovered from a difference Fourier map and subsequently refined using a riding model.

*Z-Adm-L-Ala-OMe*: Two independent molecules (**A** and **B**) in a *pseudo*-centrosymmetric arrangement (apart from the configuration of L-Ala) characterize the asymmetric unit. In both molecules, the -Ala-OMe moiety is disordered and was refined on two sets of positions with population parameters of 0.70 for the major conformers (atoms C2B, C2, O2, OTA and CTA in molecule **A**, while C4B, C4, O4, OTB and CTB in molecule **B**) and of 0.30 for the minor conformers (atoms C2B′, C2′, O2′, OTA′ and CTA′ in molecule **A**, while C4B′, C4′, O4′, OTB′ and CTB′ in molecule **B**). Restraints were applied to the bond distances and bond angles involving the disordered atoms, as well as to the anisotropic displacement parameters of the latter ones.

*N,N′-bis[(Adm)$_2$-NHiPr]-oxalamide methanol bis-solvate*: The structure is *pseudo*-centrosymmetric. The two halves of the molecule are related trough a pseudo-inversion centre located at the midpoint of the C0A-C0B bond. Although the differences in the absolute values of the corresponding torsion angles of the peptide backbone in the two halves are small (< 5.5°), the dispositions of the two terminal isopropyl groups are different and not amenable to a centrosymmetric arrangement. Indeed, the structure was originally solved in space group P-1 with half molecule as the asymmetric unit, but the refinement was unsatisfactory, particularly at the level of the terminal isopropyl group. Therefore, space group P1 was chosen.

*H-(Adm)$_2$-NHiPr*: The positional parameters of the H-atoms of the free, N-terminal amino group were recovered from a difference Fourier map and subsequently refined with the N-H distances restrained to 0.89(1) Å.

## Conformational Energy Calculations

Density Functional Theory (DFT) calculations on Ac-$(Adm)_2$-NHMe, Ac-$(c_3Dip)_2$-NHMe, and Ac-$(Ac_6c)_2$-NHMe were performed in the gas phase using the Gaussian 09 computer package [96]. The geometries of the different investigated systems were fully optimized without symmetry restrictions using the B3LYP [97,98] functional combined with the 6-31+G(d,p) [99,100] basis set. Frequency analyses were carried out to verify the nature of the minimum state of all the optimized geometries and to calculate the zero-point vibrational energies as well as both thermal and entropic corrections, these statistical terms being used to compute the conformational Gibbs free energies in the gas phase ($\Delta G$) at 298 K.

The possible cooperative energy effects associated to the generation of a repetitive γ-turn structure was determined by calculating Ac-$(Adm)_n$-NHMe with $n$ = 1-8 arranged in an all-γ-turn conformation (*i.e.*, all Adm residues were forming a γ-turn conformation). The geometry of the homo-peptides was completely optimized using the B3LYP [97,98] functional combined with the 6-31+G(d,p) [99,100] basis set. The energy increment (EI) that results when a single residue is added to the peptide chain with the same γ-turn conformation was defined as follows:

$$EI = E[\text{Ac-}(Adm)_1\text{-NHMe}] - E[\text{Ac-}(Adm)_2\text{-NHMe}] \quad (1)$$

Then, the predicted energy ($E^{pred}$) for the $n^{th}$ homo-peptide Ac-$(Adm)_n$-NHMe in such repetitive conformation could be calculated as:

$$E^{pred}[\text{Ac-}(Adm)_n\text{-NHMe}] = (n\text{-}1)\cdot EI + E[\text{Ac-}(Adm)_1\text{-NHMe}] \quad (2)$$

The cooperative energy (CE) is defined by:

$$CE = E[\text{Ac-}(Adm)_n\text{-NHMe}] - E^{pred}[\text{Ac-}(Adm)_n\text{-NHMe}] \quad (3)$$

Accordingly, CE is negative or positive in presence of cooperative or anti-cooperative effects, respectively.


## Acknowledgements

This work was supported by MINECO-FEDER (MAT2015-69367-R) and by CSUC. Support for the research of C.A. was received through the prize "ICREA Academia" for excellence in research funded by the Generalitat de Catalunya.

## References


1 Huggins ML. The structure of fibrous proteins. *Chem. Rev.* 1943; **32**: 195-218.

2 Pauling L, Corey RB. Two hydrogen-bonded spiral configurations of the polypeptide chain. *J. Am. Chem. Soc.* 1950; **72**: 5349.

3 Pauling L, Corey RB, Branson HR. The structure of proteins. Two hydrogen-bonded helical configurations of the polypeptide chain. *Proc. Natl. Acad. Sci. USA* 1951; **37**: 205-211.

4 Pauling L, Corey RB. Atomic coordinates and structural factors for two helical configurations of polypeptide chains. *Proc. Natl. Acad. Sci. USA* 1951; **37**: 235-240.

5 Low BW. The π helix. A hydrogen bonded configuration of the polypeptide chain. *J. Am. Chem. Soc.* 1952; **74**: 5806-5807.

6 Donohue J. Hydrogen bonded helical configurations of the polypeptide chain. *Proc. Natl. Acad. Sci. USA* 1953; **39**: 470-478.

7 Ramachandran GN. Conversation in the discipline "biomolecular stereodynamics". In *Biomolecular Stereodynamics*, Vol. 2, Sarma RH (ed.). Adenine Press: Guilderland (NY), 1981; 1-36.

8 Eisenberg D. The discovery of the α-helix and β-sheet, the principal structural features of proteins. *Proc. Natl. Acad. Sci. USA* 2003; **100**: 11207-11210.

9 Toniolo C, Benedetti E. The polypeptide $3_{10}$-helix. *Trends Biochem. Sci.* 1991; **16**: 350-353.

10 Toniolo C, Crisma M, Formaggio F, Peggion C. Control of peptide conformation by the Thorpe-Ingold effect ($C^{\alpha}$-tetrasubstitution). *Biopolymers (Pept. Sci.)* 2011; **60**: 396-419.

11 Crisma M, De Zotti M, Moretto A, Peggion C, Drouillat B, Wright K, Couty F, Toniolo C, Formaggio F. Single and multiple peptide γ-turns: literature survey and recent progress. *New J. Chem.* 2015; **39**: 3208-3216.

12 Prasad H, Singh S. Existence of γ-helix in natural proteins. *Int. J. Biol. Macromol.* 1981; **3**: 242-247.

13 Subramanian E, Latitha V. γ-Helix at atomic resolution. In *Conformation in Biology*, Srinivasan R, Sarma RH (eds.). Adenine Press: Guilderland (NY), 1983; 113-118.

14 Némethy G, Printz MP. The γ-turn, a possible folded conformation of the polypeptide chain. Comparison with the β-turn. *Macromolecules* 1972; **5**: 755-758.

15 Matthews BW. The γ-turn. Evidence for a new folded conformation in proteins. *Macromolecules* 1972; **5**: 818-819.

16 Printz MP, Némethy G, Bleich H. Proposed model for angiotensin II in aqueous solution and conclusions about receptor topography. *Nat. New Biol.* 1972; **237**: 135-140.

17 Holmes MA, Matthews BW. Structure of thermolysin refined at 1.6 Å resolution. *J. Mol. Biol.* 1982; **160**: 623-629.

18 Toniolo C. Intramolecularly hydrogen-bonded peptide conformations. *CRC Crit. Rev. Biochem.* 1980; **9**: 1-44.

19 Rose GD, Gierasch LM, Smith PJ. Turns in peptides and proteins. *Adv. Protein Chem.* 1985; **37**: 1-109.

20 Milner-White EJ, Ross BM, Ismail R, Belhadj-Mostefa K, Poet R. One type of γ-turn, rather than the other, gives rise to chain-reversal in proteins. *J. Mol. Biol.* 1988; **204**: 777-782.

21 Milner-White EJ. Simulations of γ-turns in proteins. Their relation to α-helices, β-sheets and ligand binding sites. *J. Mol. Biol.* 1990; **216**: 385-397.

22 Richardson JS, Keedy DA, Richardson DC. "The plot" thickens: more data, more dimensions, more uses. In *Biomolecular Forms and Functions*, Bansal M, Srinivasan N (eds.). IISC Press: Singapore, 2013, 46-61.

23 Kalmankar NV, Ramakrishnan C, Balaram P. Sparsely populated residue conformations in protein structures. Revisiting "experimental" conformational maps. *Proteins: Struct., Funct., Bioinf.* 2014; **82**: 1101-1112.

24 Khaled MA, Urry DW, Okamoto K. The γ-turn as an independent conformational feature in solution. *Biochem. Biophys. Res. Commun.* 1976; **72**: 162-169.

25 Tsunemi M, Matsuura Y, Sakakibara S, Katsube Y. Crystal structure of an elastase-specific inhibitor elafin complexed with porcine pancreatic elastase determined at 1.9 Å resolution. *Biochemistry* 1996; **35**: 11570-11576.

26 Yang M, Culhane JC, Szewczuk LM, Gocke CB, Brautigam CA, Tomchick DR, Machius M, Cole PA, Yu H. Structural basis of histone demethylation by LSD1 revealed by suicide inactivation. *Nat. Struct. Mol. Biol.* 2007; **14**: 535-539.

27 Kinarsky L, Prakash O, Vogen SM, Nomoto M, Hollingsworth MA, Sherman S. Structural effects of O-glycosylation on a 15-residue peptide from the mucin (MUC1) core protein. *Biochemistry* 2000; **39**: 12076-12082.

28 Jiménez AI, Ballano G, Cativiela C. First observation of two consecutive γ-turns in a crystalline linear dipeptide. *Angew. Chem. Int. Edit.* 2005; **44**: 396-399.

29 Venkataram Prasad BV, Balaram P. X-Pro peptides. A theoretical study of the hydrogen bonded conformations of ($\alpha$-aminoisobutyryl-L-prolyl)$_n$ sequences. *Int. J. Biol. Macromol.* 1982; **4**: 99-102.

30 Etzkorn FA, Travins JM, Hart SA. Rare protein turns: $\gamma$-turn, helix-turn-helix, and *cis*-proline mimetics. In *Advances in Amino Acid Mimetics and Peptidomimetics*, Vol. 2, Abell A (ed.). JAI Press, Stamford, CT, 1999, 125-163.

31 Avenoza A, Campos PJ, Cativiela C, Peregrina JM, Rodriguez MA. *Ab initio* calculations for N-methyl-1-(N′-acetylamino)-*t*-2-phenylcyclohexane-*r*-1-carboxamide: a $\gamma$-turn mimetic. *Tetrahedron* 1999; **55**: 1399-1406.

32 Paglialunga-Paradisi M, Torrini I, Pagani Zecchini G, Lucente G, Gavuzzo E, Mazza F, Pochetti G. $\gamma$-Turn conformation induced by $\alpha$,$\alpha$-disubstituted amino acids with a cyclic six-membered side chain. *Tetrahedron* 1995; **51**: 2379-2386.

33 Turcotte S, Lubell WD. Crystal structure analyses of azasulfuryltripeptides reveal potential for $\gamma$-turn mimicry. *Biopolymers (Pept. Sci.)* 2015; **104**: 622-628.

34 Baruah PK, Sreedevi NK, Gonnade R, Ravindranathan S, Damodaran K, Hofmann HJ, Sanjayan GJ. Enforcing periodic secondary structures in hybrid peptides: a novel hybrid foldamer containing periodic $\gamma$-turn motifs. *J. Org. Chem.* 2007; **72**: 636-639.

35 Kuroda Y, Ueda H, Nozawa H, Ogoshi H. Adamantyl amino acid as $\gamma$-turn inducer for peptide. *Tetrahedron Lett.* 1997; **38**: 7901-7904.

36 Baxendale IR, Cheung S, Kitching MO, Ley SV, Shearman JW. The synthesis of neurotensin antagonist SR 48692 for prostate cancer research. *Bioorg. Med. Chem.* 2013; **21**: 4378-4387.

37 Nagasawa HT, Elberling JA, Shirota FN. 2-Aminoadamantane-2-carboxylic acid, a rigid, achiral, tricyclic $\alpha$-amino acid with transport inhibitory properties. *J. Med. Chem.* 1973; **16**: 823-826.

38 Paventi A, Chubb FL, Edward JT. Assisted hydrolysis of the nitrile group of 2-adamantane-2-carbonitrile. *Can. J. Chem.* 1987; **65**: 2114-2117.

39 Battilocchio C, Baxendale IR, Biava M, Kitching MO, Ley SV. A flow-based synthesis of 2-aminoadamantane-2-carboxylic acid. *Org. Process Res. Dev.* 2012; **16**: 798-810.

40 Ingham RJ, Battilocchio C, Fitzpatrick DE, Sliwinski E, Hawkins JM, Ley SV. A systems approach towards an intelligent and self-controlling platform for integrated continuous reaction sequences. *Angew. Chem. Int. Edit.* 2015; **54**: 144-148.

41 Peggion C, Moretto A, Formaggio F, Crisma M, Toniolo C. Multiple, consecutive, fully-extended $2.0_5$-helix peptide conformation. *Biopolymers (Pept. Sci.)* 2013; **100**: 621-636.

42 Chacko KK, Zand R. Crystal and molecular structure of 2-aminoadamantane-2-carboxylic acid hydrochloride. *Acta Crystallogr.* 1973; **B29**: 2681-2686.

43 Kling RC, Plomer M, Lang C, Banerjee A, Hübner H, Gmeiner P. Development of covalent ligand-receptor pairs to study the binding properties of nonpeptidic neurotensin receptor 1 antagonists. *ACS Chem. Biol.* 2016; **11**: 869-875.

44 Quéré L, Boigegrain R, Jeanjean F, Gully D, Evrard G, Durant F. Structural requirements of non-peptide neurotensin receptor anatagonists. *J. Chem. Soc., Perkin Trans. 2* 1996; 2639-2646.

45 Quéré L, Longfils G, Boigegrain R, Labeeuw B, Gully D, Durant F. X-Ray structural characterization of SR 142948, a novel potent synthetic neurotensin receptor antagonist. *Bioorg. Med. Chem. Lett.* 1998; **8**: 653-658.

46 Džolić Z, Margeta R, Vinković M, Štefanic Z, Kojić-Pradić B, Mlinarić-Majerski K, Žinić M. N-Methylation of adamantane-substituted oxalamide unit affects its conformational rigidity. A skew conformation of the oxalamide bridge. *J. Mol. Struct.* 2008; **876**: 218-224.

47 Battilocchio C, Deadman BJ, Nikbin N, Kitching MO, Baxendale IR. A machine-assisted flow synthesis of SR48692: a probe for the investigation of neurotensin receptor-1. *Chem. Eur. J.* 2013; **19**: 7917-7930.

48 Makatini M, Chetty T, Onajole OK, Govender T, Govender P, Maguire GEM, Kruger HG. Synthesis and NMR elucidation of novel tetrapeptides. *J. Pept. Sci.* 2012; **18**: 114-121.

49 Marchand AP. Diamondoid hydrocarbons. Delving into Nature's bounty. *Science* 2003; **299**: 52-53.

50 Zaworodko ML. Crystal engineering of diamondoid networks. *Chem. Soc. Rev.* 1994; **23**: 283-288.

51 Gunawan MA, Hierso JC, Poinsot D, Fokin AA, Fokina NA, Tkachenko BA, Schreiner PR. Diamondoids: functionalization and subsequent applications of perfectly defined molecular cage hydrocarbons. *New J. Chem.* 2014; **38**: 28-41.

52 Dahl JE, Liu SG, Carlson RMK. Isolation and structure of higher diamondoids, nanometer-sized diamond molecules. *Science* 2003; **299**: 96-99.

53 von R. Schleyer P. A simple preparation of adamantane. *J. Am. Chem. Soc.* 1957; **79**: 3292.

54 von R. Schleyer P. My thirty years in hydrocarbon cages: from adamantane to dodecahedrane. In *Cage Hydrocarbons*, Olah GH (ed.). Wiley, New York (NY), 1990, 1-38.

55 Schaefer HF. Paul von Ragué Schleyer (obituary). *Nature* 2015; **517**: 22.

56 Thomas JB, Giddings AM, Olepu S, Wiethe RW, Warner KR, Sarret P, Longpre JM, Runyon SP, Gilmour BP. The amide linker in nonpeptide neurotensin receptor ligands plays a key role in calcium signaling at the neurotensin receptor type 2. *Bioorg. Med. Chem. Lett.* 2015; **25**: 2060-2064.

57 Szczesniack P, Pieczykolan M, Stecko S. The synthesis of α,α-disubstituted α-amino acids via Ichikawa rearrangement. *J. Org. Chem.*2016; **81**: 1057-1074.

58 Gully D, Canton M, Boigegrain R, Jeanjean F, Molimard JC, Poncelet M, Gueudet C, Heaulme M, Leyris R, Bronard A, Pelaprat D, Labbé-Jullié C, Mazella J, Soubrié P, Maffrand JP, Rostène W, Kitalgi P, Le Fur G. Biochemical and pharmacological profile of a potent and selective nonpeptide antagonist of the neurotensin receptor. *Proc. Natl. Acad. Sci. USA* 1993; **90**: 65-69.

59 Chubb FL, Edward JT, Wong SC. Simplex optimization of yields in the Bucherer-Bergs reaction. *J. Org. Chem.* 1980; **45**: 2315-2320.

60 Nagasawa HT, Elberling JA, Shirota FN. Potential latentiation forms of biologically active compounds based on action of leucine aminopeptidase. Dipeptide derivatives of the tricycloaliphatic α-amino acid, adamantanine. *J. Med. Chem.* 1975; **18**: 826-830.

61 Carpino LA. 1-Hydroxy-7-azabenzotriazole. An efficient peptide coupling additive. *J. Am. Chem. Soc.* 1993; **115**: 4397-4398.

62 Adams R, Ulich LH. The use of oxalyl chloride and bromide for producing acid chlorides, acid bromides or acid anhydrides. *J. Am. Chem. Soc.* 1920; **42**: 599-611.

63 Bosshard HH, Mory R, Schmid M, Zollinger H. Eine Methode zur Katalysierten herstellung von Carbonsäure und Sulfosäure-chloriden mit Thionylchlorid. *Helv. Chim. Acta* 1959; **42**: 1653-1658.

64 Montalbetti CAGN, Falque V. Amide bond formation and peptide coupling. *Tetrahedron* 2005; **61**: 10827-10852.

65 Jones JE, Diemer V, Adam C, Raftery J, Ruscoe RE, Sengel JT, Wallace MI, Bader A, Cockroft SL, Clayden J, Webb SJ. Length-dependent formation of transmembrane pores by $3_{10}$-helical α-aminoisobutyric acid foldamers. *J. Am. Chem. Soc.* 2016; **138**: 688-695.

66 Meldal M, Juliano MA, Jansson AM. Azido acids in a novel method of solid-phase peptide synthesis. *Tetrahedron Lett.* 1997; **38**: 2531-2534.

67 Meldal M, Renil M, Juliano MA, Jansson AM, Meinjohanns E, Buchardt J, Schleyer A. Novel PEG-based resins and synthetic methods. Azido acids in SPPS and direct solid-phase

peptide glycosylations. In *Peptides 1996*, Ramage R, Epton R (eds.). Mayflower Scientific, Kingswinford (UK), 1998, 141-152.

68 Tornoe C, Christensen C, Meldal M. Peptidotriazoles on solid phase: [1,2,3]-triazole by regiospecific copper(I)-catalyzed 1,3-dipolar cycloadditions of terminal alkynes to azides. *J. Org. Chem.* 2002; **67**: 3057-3064.

69 Benedetti E, Pedone C, Toniolo C, Sudek M, Némethy G, Scheraga HA. Preferred conformation of the benzyloxycarbonyl-amino group in peptides. *Int. J. Pept. Protein Res.* 1983; **21**: 163-181.

70 Chen CS, Parthasarathy R. Specific configurations of hydrogen bonding. I. Hydrogen bond and conformational preferences of N-acylamino acids, peptides and derivatives. Int. J. Pept. Protein Res. 1978; **11**: 9-18.

71 Chakrabarti P, Dunitz JD. Structural characteristics of the carboxylic amide group. Helv. Chim. Acta 1982; **65**: 1555-1562.

72 Schweizer WB, Dunitz JD. Structural characteristics of the carboxylic ester group. Helv. Chim. Acta 1982; **65**: 1547-1554.

73 Allen FH, Kennard O, Watson DG, Brammer L, Orpen AG, Taylor R. Tables of bond lengths determined by X-ray and neutron diffraction. Part I. Bond lengths in organic compounds. *J. Chem. Soc., Perkin Trans. II* 1987; S1-S19.

74 Benedetti E. In *Chemistry and Biochemistry of Amino Acids, Peptides and Proteins*, Vol. 6, Weinstein B (ed.). Dekker: New York, 1982; 105-184.

75 Ashida T, Tsunogae Y, Tanaka I, Yamane T. Peptide chain structure parameters, bond angles and conformational angles from the Cambridge Structural Database. *Acta Crystallogr.* 1987; **B43**: 212-218.

76 Ramakrishnan C, Prasad N. Study of hydrogen bonds in amino acids and peptides. *Int. J. Pept. Protein Res.* 1971; **3**: 209-231.

77 Taylor R, Kennard O, Versichel W. The geometry of the N-H…O=C hydrogen bond. 3. Hydrogen-bond distances and angles. *Acta Crystallogr.* 1984; **B40**: 280-288.

78 Görbitz CH. Hydrogen bond distances and angles in the structures of amino acids and peptides. *Acta Crystallogr.* 1989; **B45**: 390-395.

79 Torshin IY, Weber IT, Harrosin RW. Geometric criteria of hydrogen bonds in proteins and identification of “bifurcated” hydrogen bonds. *Protein Eng.* 2002; **15**: 359-363.

80 Zimmerman SS, Pottle MS, Némethy G, Scheraga HA. Conformational analysis of the 20 naturally occurring amino acid residues using ECEPP. *Macromolecules* 1977; **10**: 1-9.

81 Crisma M, Formaggio F, Moretto A, Toniolo C. Peptide helices based on α-amino acids. *Biopolymers (Pept. Sci.)* 2006; **84**: 3-12.

82 Paterson Y, Rumsey SM, Benedetti E, Némethy G, Scheraga HA. Sensitivity of polypeptide conformation to geometry. Theoretical conformational analysis of oligomers of α-aminoisobutyric acid. *J. Am. Chem. Soc.* 1981; **103**: 2947-2955.

83 Zanuy D, Alemán C. Modeling of the α-helical conformation of homopeptides constituted by α-L-glutamic acid. *Biopolymers* 1999; **49**: 497-504.

84 Alemán C, Casanovas J, Galembeck SE. PAPQMD parametrization of molecular systems with cyclopropyl rings. Conformational study of homo-peptides constituted by 1-aminocyclopropane-1-carboxylic acid. *J. Comput. Aided Mol. Design.* 1998; **12**: 259-273.

85 Alemán C, Roca R, Luque FJ, Orozco M. Helical preferences of alanine, glycine, and aminoisobutyric homopeptides. *Proteins: Struct. Funct. Genet.* 1997; **28**: 83-93.

86 Venkatachalam CM. Stereochemical criteria for polypeptides and proteins. V. Conformation of a system of three-linked peptide units. *Biopolymers* 1968; **6**: 1425-1436.

87 Casanovas J, Jiménez AI, Cativiela C, Pérez JJ, Alemán C. Conformational analysis of a cyclopropane analogue of phenylalanine with two geminal phenyl substituents. *J. Phys. Chem. B* 2006; **110**: 5762-5766.

88 Zanuy D, Jiménez AI, Cativiela C, Nussinov R, Alemán C. Use of synthetic constrained amino acids in β-helix proteins for conformational control. *J. Phys. Chem. B* 2007; **111**: 3236-3242.

89 Goddard-Borger ED, Stick RV. An efficient, inexpensive, and shelf-stable diazotransfer reagent: imidazole-1-sulfonylazide hydrochloride. *Org. Lett.* 2007; **9**: 3797-3800.

90 Anderson GW, Zimmerman JE, Callahan FM. N-Hydroxysuccinimide esters in peptide synthesis. *J. Am. Chem. Soc.* 1963; **85**: 3039.

91 Paquet A. Introduction of 9-fluorenylmethoxycarbonyl, trichloroethoxycarbonyl, and benzyloxycarbonyl amino protecting groups into O-unprotected hydroxy amino acids using succinimidyl carbonates. *Can. J. Chem.* 1982; **60**: 981-989.

92 Burla MC, Camalli M, Carrozzini B, Cascarano GL, Giacovazzo C, Polidori G, Spagna R. SIR2002: the program. *J. Appl. Crystallogr.* 2003, **36**: 1103.

93 Burla MC, Caliandro R, Carrozzini B, Cascarano GL, Cuocci C, Giacovazzo C, Mallamo M, Mazzone A, Polidori G. Crystal structure determination and refinement *via* SIR2014. *J. Appl. Crystallogr.* 2015, **48**: 306-309.

94 Sheldrick GM. A short history of SHELX. *Acta Crystallogr.* 2008, **A64**: 112-122.

95 Sheldrick GM. Crystal structure refinement with SHELXL. *Acta Crystallogr.* 2015, **C71**: 3-8.

96 Frisch MJ, Trucks GW, Schlegel HB, Scuseria GE, Robb MA, Cheeseman JR, Scalmani G, Barone V, Mennucci B, Petersson GA, Nakatsuji H, Caricato M, Li X, Hratchian HP, Izmaylov AF, Bloino J, Zheng G, Sonnenberg JL, Hada M, Ehara M, Toyota K, Fukuda R, Hasegawa J, Ishida M, Nakajima T, Honda Y, Kitao O, Nakai H, Vreven T, Montgomery JA Jr, Peralta JE, Ogliaro F, Bearpark M, Heyd JJ, Brothers E, Kudin KN, Staroverov VN, Kobayashi R, Normand J, Raghavachari K, Rendell A, Burant JC, Iyengar SS, Tomasi J, Cossi M, Rega N, Millam JM, Klene M, Knox JE, Cross JB, Bakken V, Adamo C, Jaramillo J, Gomperts R, Stratmann RE, Yazyev O, Austin AJ, Cammi R, Pomelli C, Ochterski JW, Martin RL, Morokuma K, Zakrzewski VG, Voth GA, Salvador P, Dannenberg JJ, Dapprich S, Daniels AD, Farkas O, Foresman JB, Ortiz JV, Cioslowski J, Fox DJ. *Gaussian 09, revision A.01*, Gaussian, Inc.: Wallingford, CT, 2009.

97 Becke AD. A new mixing of Hartree-Fock and local density-functional theories. *J. Chem. Phys.* 1993; **98**: 1372-1377.

98 Lee C, Yang W, Parr RG. Development of the Colle-Salvetti correlation-energy formula into a functional of the election density. *Phys. Rev. B* 1988; **37**: 785-789.

99 Hariharan PC, Pople JA. The influence of polarization functions on molecular orbital hydrogenation energies. *Theor. Chim. Acta* 1973; **28**: 213-222.

100 McLean AD, Chandler GS. Contracted Gaussian basis sets for molecular calculations. I. Second row atoms, $Z$ = 11-18. *J. Chem. Phys.* 1980; **72**: 5639-5648.

## Supporting information

Additional supporting information may be found in the online version of this article at the publisher's web site.

Tables S1-S12. Crystal data and structure refinement parameters for the thirteen X-ray diffraction structures described in this work.

**Table 1.** Backbone torsion angles (°) involving the amino acid residues from the X-ray diffraction structures solved in this work

| Compound | $\omega_0$ | $\phi_1$ | $\psi_1$ | $\omega_1$ | $\phi_2$ | $\psi_2$ | $\omega_2$ | $\phi_3$ | $\psi_3$ | $\omega_3$ |
|---|---|---|---|---|---|---|---|---|---|---|
| 0. "$N_3$"-Adm-NH*i*Pr | | | -92.80(14) | 173.48(13) | | | | | | |
| 1. Z-Adm-OH | 179.96(12) | -57.44(15) | -50.52(14)[a] | | | | | | | |
| 2. Z-Adm-NH*i*Pr | 178.05(12) | -72.22(15) | 91.66(14)[b] | -170.58(14)[c] | | | | | | |
| 3. N,N′-*bis*- [$(Adm)_2$-NH*i*Pr] oxalamide | 173.7(4)[d]<br>-173.2(5)[g] | -74.5(6)<br>73.1(6) | 85.9(5)<br>-80.4(5) | 179.3(4)<br>-180.0(4) | -69.3(6)<br>65.6(6) | 97.9(6)[e]<br>-100.8(6)[h] | -176.3(5)[f]<br>172.3(6)[i] | | | |
| 4. Z-Adm-Gly-OEt | 173.70(11) | -72.85(14) | 98.50(12) | 177.20(12) | 77.93(17) | -172.00(13)[j] | 179.37(19)[k] | | | |
| 5. Z-Adm-L-Ala-OMe | | | | | | | | | | |
| molecule **A** | -165.0(5) | 69.4(7) | -94.5(6) | 178.8(5) | 42.5(9)<br>[66(2)][l] | 48.8(10)[m]<br>[33(5)][l] | -179.3(10)[n]<br>[-174(5)][l] | | | |
| molecule **B** | 164.4(5) | -70.6(6) | 93.9(6) | 179.1(5) | -45.0(10)<br>[-92.4(8)][l] | -47.2(11)[o]<br>[12.1(5)][l] | -173.8(10)[p]<br>[164.6(5)][l] | | | |
| 6. H-$(Adm)_2$-NH*i*Pr | | | -71.4(3) | 173.8(3) | -80.5(4) | 96.1(3)[q] | -169.9(3)[r] | | | |
| 7. "$N_3$"-$(Adm)_2$-NH*i*Pr | | | -81.6(2) | 167.56(16) | -79.0(2) | 94.88(19)[q] | 179.5(2)[r] | | | |
| 8. Tfa-$(Adm)_2$-NH*i*Pr | 176.0(2) | -78.7(3) | 88.1(2) | 179.1(2) | -60.8(3) | -65.5(2)[q] | 178.3(2)[r] | | | |
| 9. "$N_3$"-$(Adm)_3$-NH*i*Pr | | | 77.87(17) | -171.21(13) | -81.91(18) | 84.20(16) | 173.57(13) | -72.98(19) | 75.88(18)[s] | -179.85(15)[t] |

[a]N1-C1A-C1-OT. [b]N1-C1A-C1-NT. [c]C1A-C1-NT-CT1. [d]C0B-C0A-N1-C1A. [e]N2-C2A-C2-NTA. [f]C2A-C2-NTA-CT1A. [g]C0A-C0B-N3-C3A.

*(ctd)*

*ctd*

[h]N4-C4A-C4-NTB. [i]C4A-C4-NTB-CT1B. [j]N2-C2A-C2-OT. [k]C2A-C2-OT-CT1. [l]The value in square brackets refers to the minor occupancy site of the -L-Ala-OMe moiety. [m]N2-C2A-C2-OTA. [n]C2A-C2-OTA-CTA. [o]N4-C4A-C4-OTB. [p]C4A-C4-OTB-CTB. [q]N2-C2A-C2-NT. [r]C2A-C2-NT-CT1. [s]N3-C3A-C3-NT. [t]C3A-C3-NT-CT1.

**Table 2.** Intra- and intermolecular H-bond parameters for the Adm derivatives and peptides investigated in this work by X-ray diffraction

| Compound | Type | Donor D-H | Acceptor A | Distance (Å) D…A | Distance (Å) H…A | Angle (°) D-H…A | Symmetry equivalence of A |
|---|---|---|---|---|---|---|---|
| 0. "$N_3$"-Adm-NH*i*Pr | Intermolecular | NT-HT | O1 | 2.9062(14) | 2.12 | 152 | *x*, -*y*, *z*+1/2 |
| 1. Z-Adm-OH | Intermolecular | N1-H1 | OT | 3.1620(15) | 2.40 | 147 | -*x*+2, -*y*+1, -*z* |
| | Intermolecular | OT-HT | O0 | 2.6705(14) | 1.86 | 172 | -*x*+2, -*y*, -*z* |
| 2. Z-Adm-NH*i*Pr | Open γ-turn | NT-HT | O0 | 3.0451(17) | 2.70 | 105 | *x*, *y*, *z* |
| | Intermolecular | N1-H1 | O1 | 2.9117(16) | 2.10 | 158 | -*x*+1, -*y*, -*z* |
| | Intermolecular | NT-HT | O0 | 3.1886(16) | 2.37 | 158 | -*x*+1, -*y*+1, -*z* |
| 3. N,N′-*bis*[$(Adm)_2$-NH*i*Pr] oxalamide methanol *bis*-solvate | γ-Turn | N2-H2 | O0A | 3.009(6) | 2.45 | 123 | *x*, *y*, *z* |
| | Open γ-turn | NTA-HTA | O1 | 3.038(7) | 2.78 | 99 | *x*, *y*, *z* |
| | γ-Turn | N4-H4 | O0B | 2.996(6) | 2.40 | 126 | *x*, *y*, *z* |
| | Open γ-turn | NTB-HTB | O3 | 3.008(7) | 2.77 | 98 | *x*, *y*, *z* |
| | Intermolecular | NTA-HTA | O3 | 3.232(7) | 2.40 | 163 | *x*, *y*+1, *z* |
| | Intermolecular | NTB-HTB | O1 | 3.109(8) | 2.38 | 142 | *x*, *y*-1, *z* |
| | Solvent-peptide | O1M-H1M | O2 | 2.792(9) | 2.00 | 161 | *x*, *y*, *z* |
| | Solvent-peptide | O2M-H2M | O4 | 2.732(11) | 1.93 | 166 | *x*, *y*, *z* |

*(ctd)*

*ctd*

| | | | | | | | |
|---|---|---|---|---|---|---|---|
| 4. Z-Adm-Gly-OEt | Open γ-turn | N2-H2 | O0 | 3.1502(15) | 2.74 | 111 | *x*, *y*, *z* |
| | Intermolecular | N1-H1 | O1 | 2.9831(14) | 2.17 | 159 | -*x*+1, -*y*, -*z* |
| | Intermolecular | N2-H2 | O0 | 2.8647(15) | 2.12 | 144 | -*x*+1, -*y*+1, -*z* |
| 5. Z-Adm-L-Ala-OMe | Open γ-turn | N2-H2 | O0A | 3.124(9) | 2.71 | 111 | *x*, *y*, *z* |
| | Open γ-turn | N4-H4 | O0B | 3.179(8) | 2.75 | 113 | *x*, *y*, *z* |
| | Intermolecular | N1-H1 | O3 | 2.879(6) | 2.07 | 157 | *x*, *y*, *z* |
| | Intermolecular | N2-H2 | O0B | 2.908(7) | 2.14 | 149 | *x*+1, *y*, *z* |
| | Intermolecular | N3-H3 | O1 | 2.980(6) | 2.18 | 155 | *x*, *y*, *z* |
| | Intermolecular | N4-H4 | O0A | 3.038(6) | 2.21 | 161 | *x*-1, *y*, *z* |
| 6. H-$(Adm)_2$-NH*i*Pr | Open γ-turn | NT-HT | O1 | 3.293(4) | 2.97 | 105 | *x*, *y*, *z* |
| | Intermolecular | N1-H1A | O2 | 3.131(4) | 2.25 | 170 | -*x*, -*y*, -*z* |
| | Intermolecular | N2-H2 | O2 | 3.152(3) | 2.44 | 141 | -*x*, -*y*, -*z* |
| | Intermolecular | NT-HT | O1 | 2.997(4) | 2.21 | 152 | -*x*+1, -*y*, -*z* |
| 7. "$N_3$"-$(Adm)_2$-NH*i*Pr | Open γ-turn | NT-HT | O1 | 3.232(2) | 2.76 | 116 | *x*, *y*, *z* |
| | Intermolecular | N2-H2 | O2 | 3.170(2) | 2.38 | 153 | -*x*+2, -*y*+1, -*z* |
| | Intermolecular | NT-HT | O1 | 3.178(3) | 2.38 | 154 | -*x*+2, -*y*, -*z* |

*(ctd)*

*ctd*

| | | | | | | | |
|---|---|---|---|---|---|---|---|
| 8. Tfa-$(Adm)_2$-NH*i*Pr | γ-Turn | N2-H2 | O0 | 3.091(3) | 2.54 | 123 | *x*, *y*, *z* |
| | Intermolecular | N1-H1 | O1 | 2.940(3) | 2.11 | 162 | -*x*, -*y*, -*z*+1 |
| | Intermolecular | NT-HT | O2 | 3.477(3) | 2.66 | 158 | -*x*+1/2, *y*-1/2, -*z*+3/2 |
| 9. "$N_3$"-$(Adm)_3$-NH*i*Pr | γ-Turn | N3-H3 | O1 | 3.0792(19) | 2.44 | 132 | *x*, *y*, *z* |
| | γ-Turn | NT-HT | O2 | 2.912(2) | 2.27 | 132 | *x*, *y*, *z* |

**Table 3.** Average bond angles (°) at $C^{\alpha}$ for the Adm residue in different backbone conformations for the peptides investigated in this work by X-ray diffraction

| | N-$C^{\alpha}$-C′ [a] | N-$C^{\alpha}$-$C^{\beta1}$ [b] | N-$C^{\alpha}$-$C^{\beta2}$ | C′-$C^{\alpha}$-$C^{\beta1}$ | C′-$C^{\alpha}$-$C^{\beta2}$ | $C^{\beta1}$-$C^{\alpha}$-$C^{\beta2}$ |
|---|---|---|---|---|---|---|
| γ-turn / open γ-turn (ϕ negative, ψ positive) | 104.5 | 107.4 | 112.7 | 109.6 | 114.8 | 107.6 |
| helical (right-handed) | 106.9 | 106.9 | 112.2 | 111.4 | 111.4 | 108.2 |

[a]Also termed τ. [b] $C^{\beta1}$, (*pro-S*)-$C^{\beta}$; $C^{\beta2}$, (*pro-R*)-$C^{\beta}$.

**Table 4.** Results from the DFT conformational energy calculations for the N-acetylated Adm, $c_3$Dip, and $Ac_6c$ homo-dipeptide methylamides in the gas phase at the B3LYP/6-31+G(d,p) level [a]

| $\omega_0$ | $\varphi_1$ | $\psi_1$ | $\omega_1$ | $\varphi_2$ | $\psi_2$ | $\omega_2$ | $\Delta E$ | $\Delta G$ | Conformation |
|---|---|---|---|---|---|---|---|---|---|
| | | | | | Ac-$(Adm)_2$-NHMe | | | | |
| -179.5 | -77.8 | 74.9 | 179.3 | -72.4 | 77.4 | -174.3 | 0.0 | 0.0 | two consecutive γ-turns |
| -179.9 | -70.0 | 89.6 | -170.1 | 60.1 | 49.4 | 179.5 | 2.7 | 2.6 | distorted β-turn (type-II) |
| -169.6 | -62.6 | -31.0 | -177.4 | -56.4 | -36.6 | -178.0 | 4.1 | 4.5 | β-turn (type-III) |
| | | | | | Ac-$(c_3Dip)_2$-NHMe | | | | |
| 174.5 | 72.6 | -47.3 | 170.0 | 72.3 | -45.1 | -179.9 | 0.0 | 0.3 | two consecutive γ-turns |
| -170.7 | -66.5 | -21.7 | 174.7 | -71.9 | -19.1 | 175.2 | 1.0 | 0.0 | β-turn (type-I) |
| | | | | | Ac-$(Ac_6c)_2$-NHMe | | | | |
| 178.3 | 54.7 | -73.9 | -179.4 | 48.2 | -75.0 | -171.8 | 0.0 | 0.4 | two consecutive γ-turns |
| -168.4 | -62.7 | -27.5 | -179.3 | -66.7 | -19.0 | -179.3 | 0.0 | 0.0 | β-turn (type-I) |

[a]Peptide torsion angles in (°); ΔE (relative energy) and ΔG (free energy) values in kcal/mol.

**FIGURE LEGENDS**

**Figure 1** Representations of the two γ-helices (or $2.2_7$-helices) generated by multiple, consecutive γ-turns of the *inverse* type (top) and *classical* type (bottom). Adapted from ref. [11].

**Figure 2** Chemical structures of the Adm and (*S*)-$c_3$Dip residues.

**Figure 3** X-Ray diffraction structure of 2-hydroxyadamantane-2-carbonitrile with numbering of the atoms. The intermolecular H-bond between the two crystallographically independent molecules (**A** and **B**) in the asymmetric unit is represented as a dashed line.

**Figure 4** X-Ray diffraction structure of "$N_3$"-Adm-NH*i*Pr with numbering of the atoms.

**Figure 5** X-Ray diffraction structure of Z-Adm-OH with numbering of the atoms.

**Figure 6** X-Ray diffraction structure of Z-Adm-NH*i*Pr with numbering of the atoms.

**Figure 7** X-Ray diffraction structure of N,N′-*bis*[$(Adm)_2$-NH*i*Pr] oxalamide with numbering of the atoms. The intramolecular H-bonds are represented by dashed lines.

**Figure 8** X-Ray diffraction structure of Z-Adm-Gly-OEt with numbering of the atoms.

**Figure 9** X-Ray diffraction structures of the two crystallographically independent molecules (**A** and **B**) in the asymmetric unit of Z-Adm-L-Ala-OMe with numbering of the atoms. In both molecules, only the major occupancy sites for the disordered -Ala-OMe moiety are shown.

**Figure 10** X-Ray diffraction structure of H-$(Adm)_2$-NH*i*Pr with numbering of the atoms.

**Figure 11** X-Ray diffraction structure of "$N_3$"-$(Adm)_2$-NH*i*Pr with numbering of the atoms.

**Figure 12** X-Ray diffraction structure of Tfa-$(Adm)_2$-NH*i*Pr with numbering of the atoms. The intramolecular H-bond is represented by a dashed line.

**Figure 13** X-Ray diffraction structure of "$N_3$"-$(Adm)_3$-NH*i*Pr with numbering of the atoms. The intramolecular H-bonds are represented by dashed lines.

**Figure 14** Left: scatterplot of the ϕ,ψ sets for the 15 N-acylated Adm residues crystallographically documented in this work, normalized to the negative sign for the ϕ torsion angle. The different conformations are highlighted according to the following color code: black, helical; red, γ-turn; blue, open γ-turn (see text for details). Right: upper left quadrant expanded.

**Figure 15** Variation of the cooperative energy (CE) with the number of amino acid residues for the γ-turn conformations of Ac-$(Adm)_n$-NHMe (*n* = 3-8). The resulting anti-cooperative effect follows a linear behavior (straight line).

**Figure 16** DFT calculated 3D-structures for Ac-$(Adm)_2$-NHMe: (**A**) two consecutive γ-turns, (**B**) distorted type-II β-turn, and (**C**) regular type-III β-turn. The H…O distances (Å) and the N-H…O angles (°) for the intramolecular H-bonds are indicated.

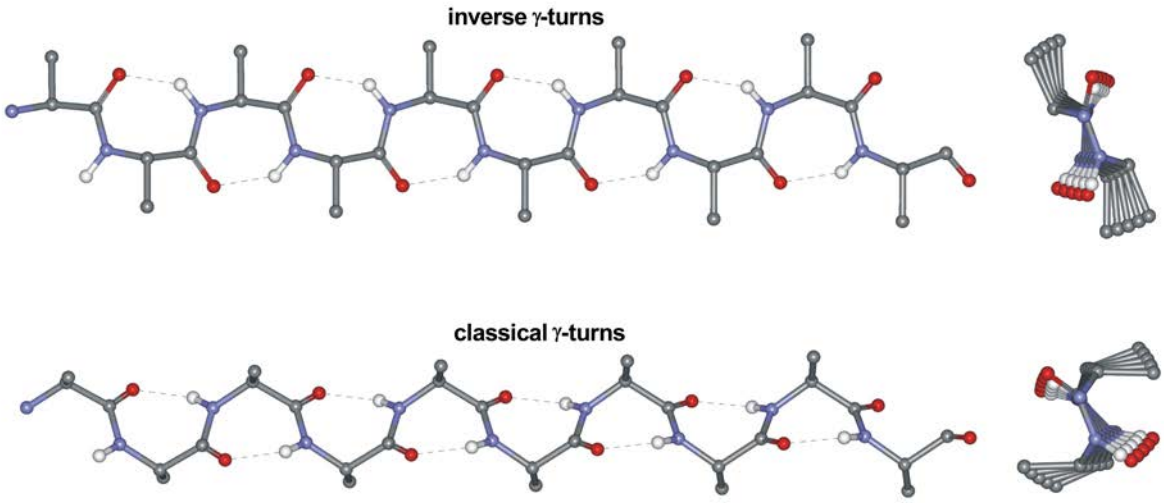


**Figure 1**

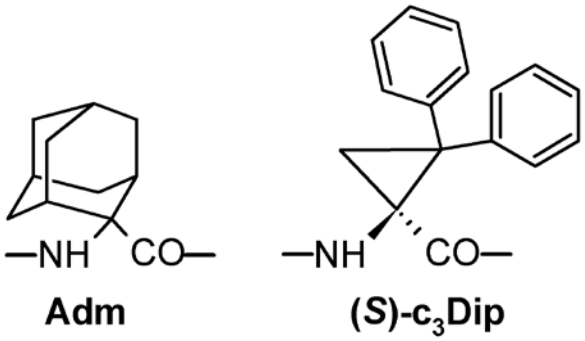


**Figure 2**

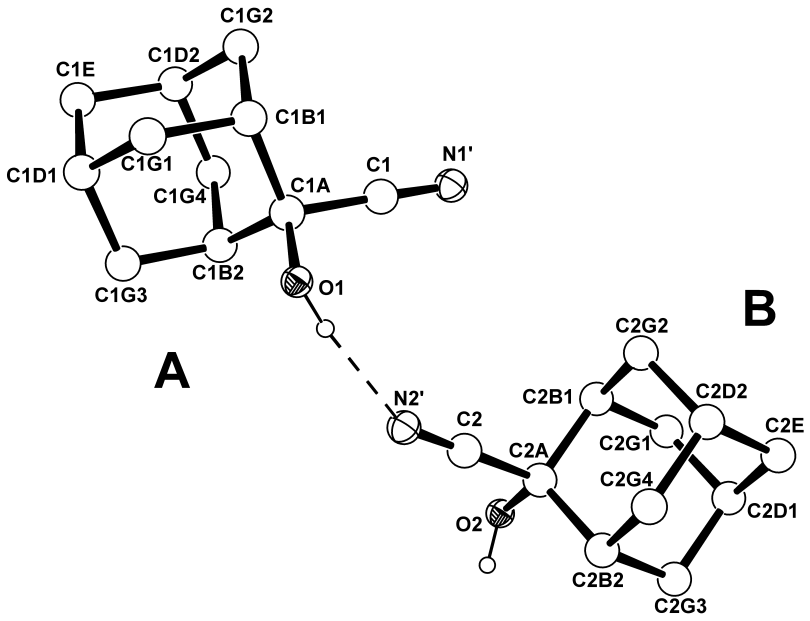


**Figure 3**

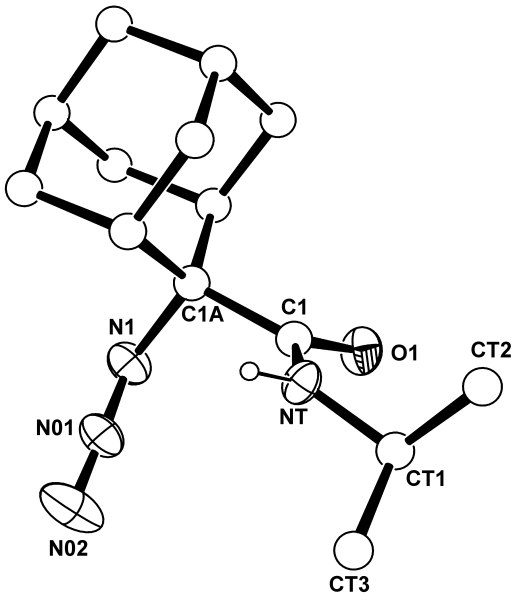


**Figure 4**

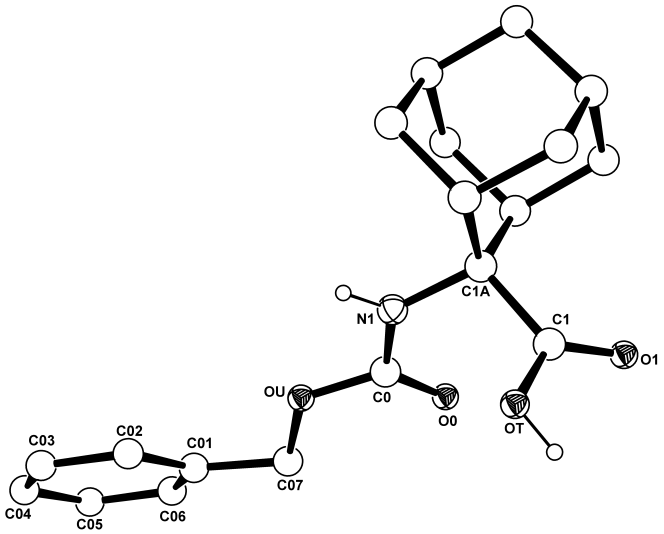


**Figure 5**

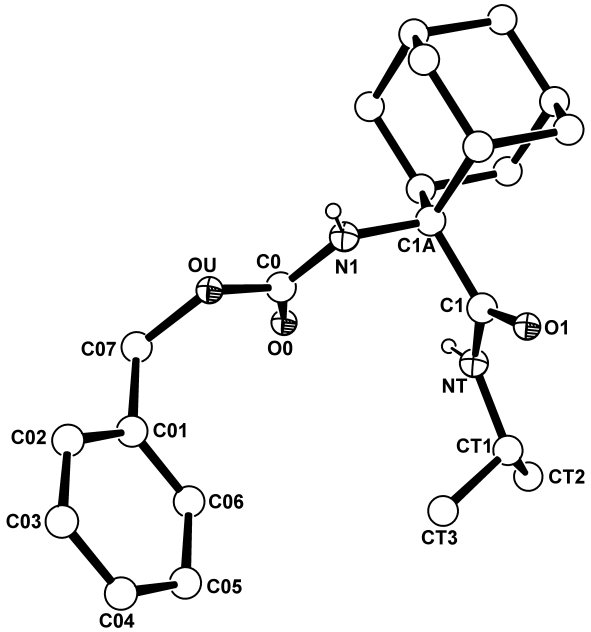


**Figure 6**

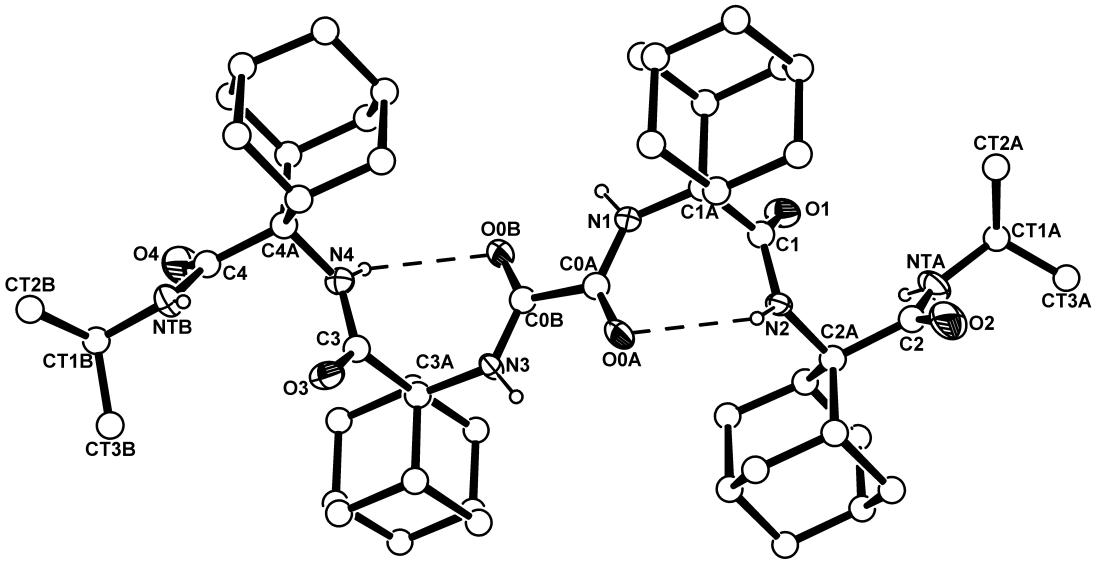
CT2A
CT1A
CT3A
NTA
O2
C2
N2
C2A
O1
C1
C1A
N1
O0B
C0A
O0A
C0B
N4
C4A
O4
C4
NTB
CT2B
CT1B
CT3B
C3
O3
C3A
N3

**Figure 7**

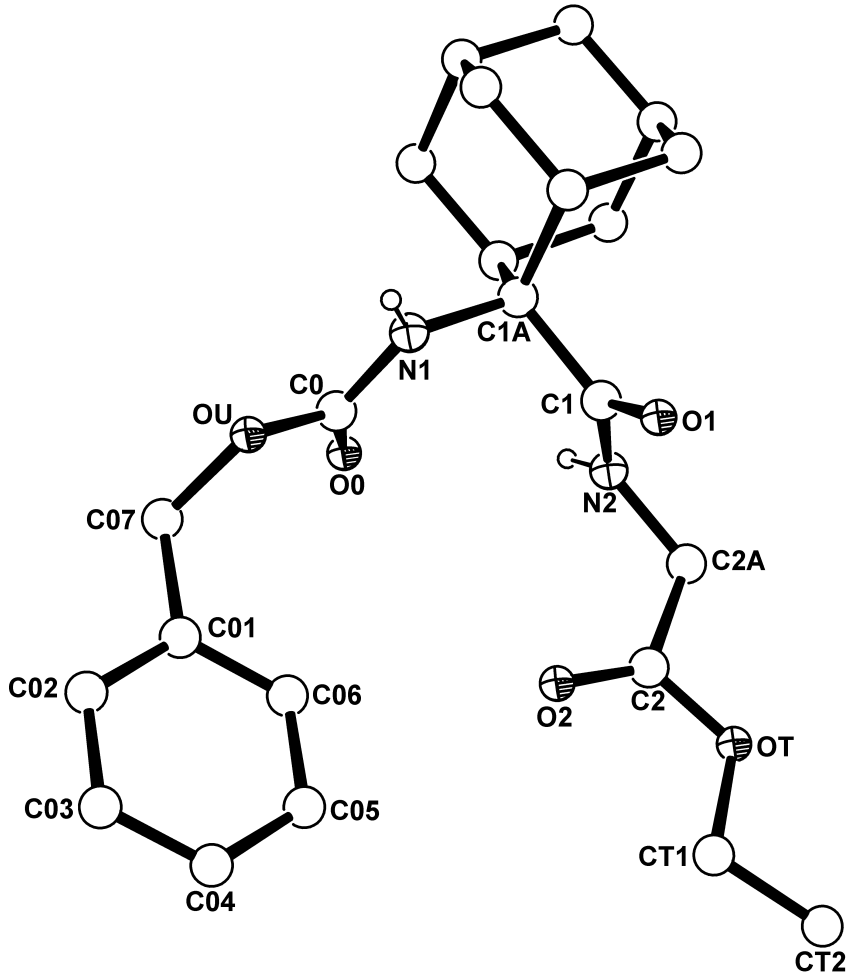
C1A
N1
C0
OU
O0
C1
O1
N2
C07
C2A
C01
C02
C06
O2
C2
OT
C03
C05
CT1
C04
CT2

**Figure 8**

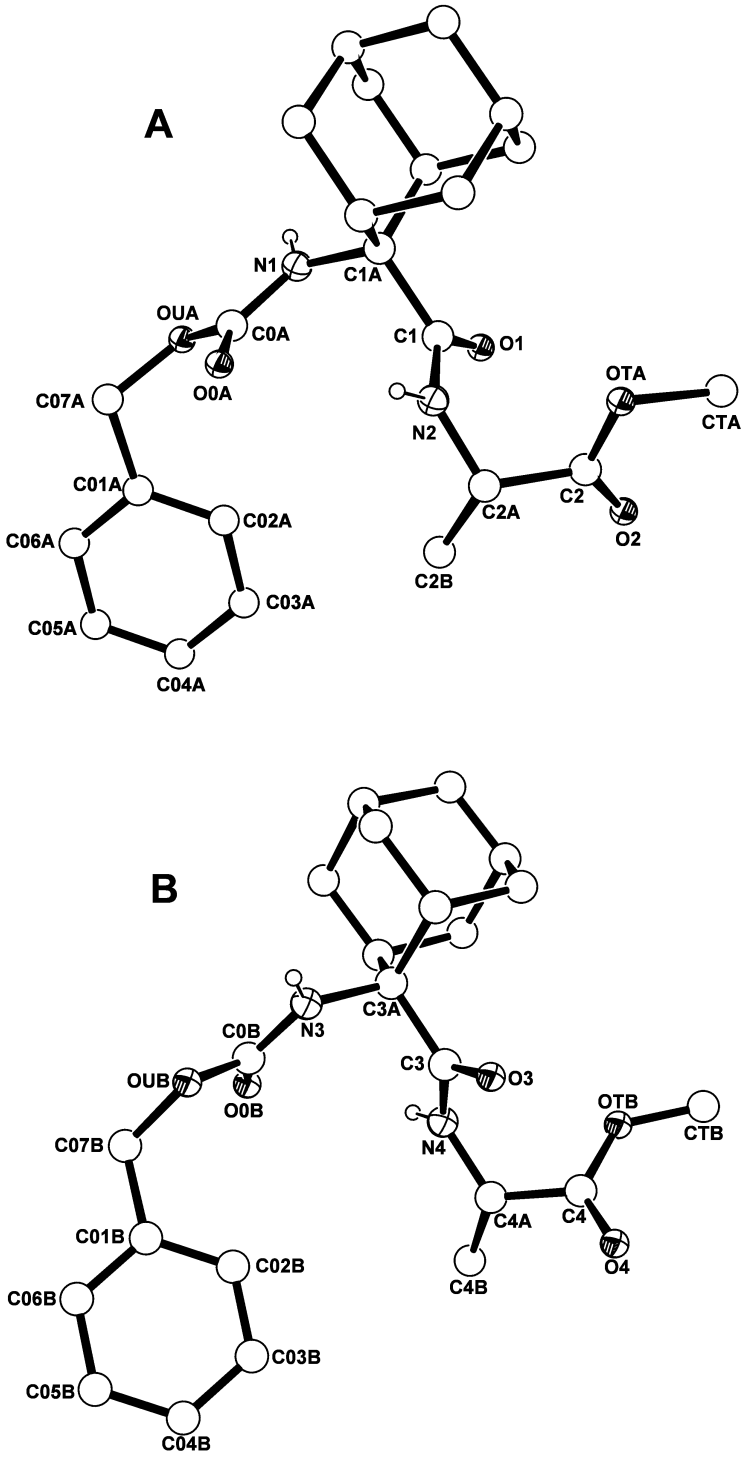
A
N1
C1A
OUA
C0A
C1
O1
O0A
OTA
C07A
N2
CTA
C01A
C2
C02A
C2A
O2
C06A
C2B
C03A
C05A
C04A
B
C3A
N3
C0B
C3
O3
OUB
O0B
OTB
CTB
C07B
N4
C4A
C4
C01B
C02B
O4
C06B
C4B
C03B
C05B
C04B

**Figure 9**

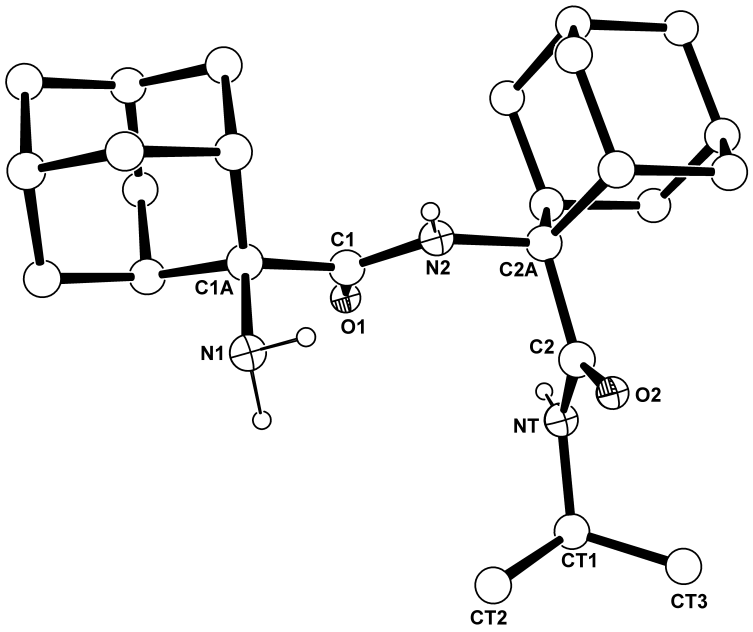


**Figure 10**

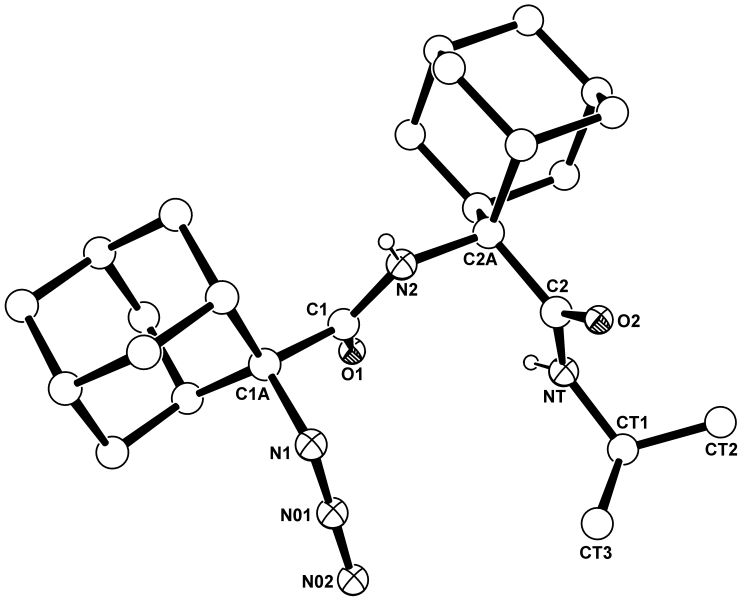


**Figure 11**

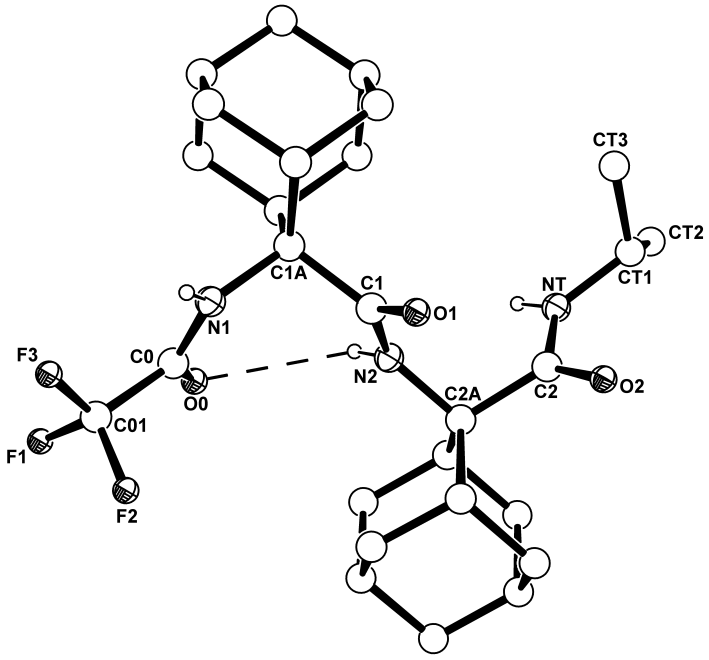


**Figure 12**

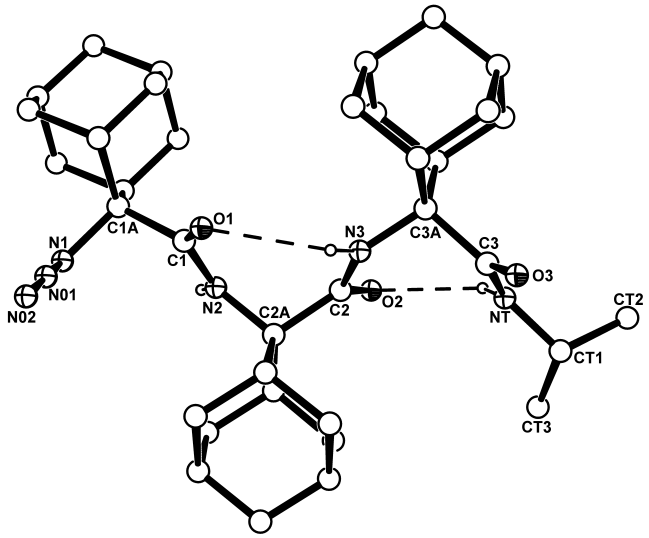


**Figure 13**

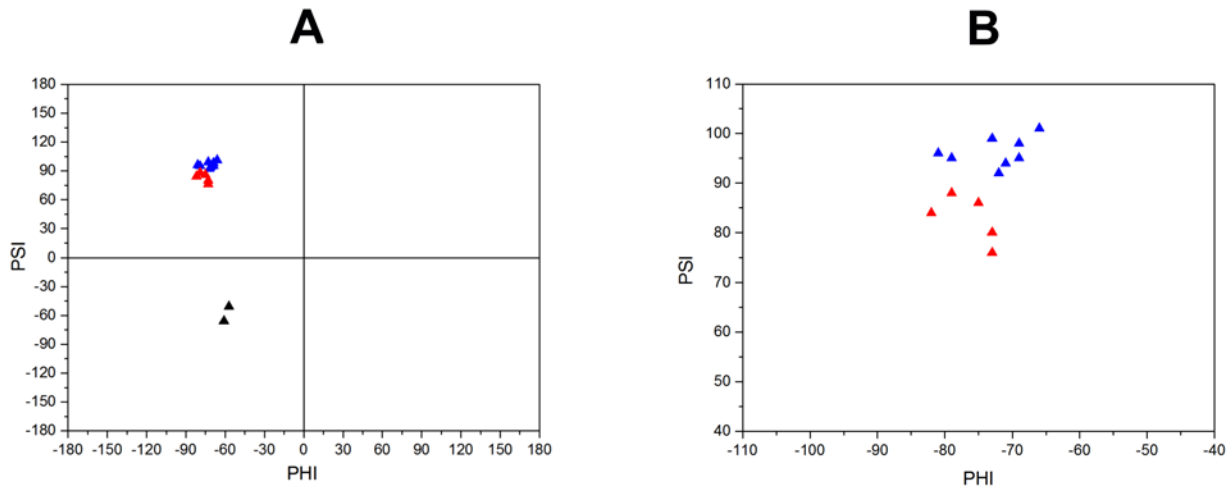


**Figure 14**

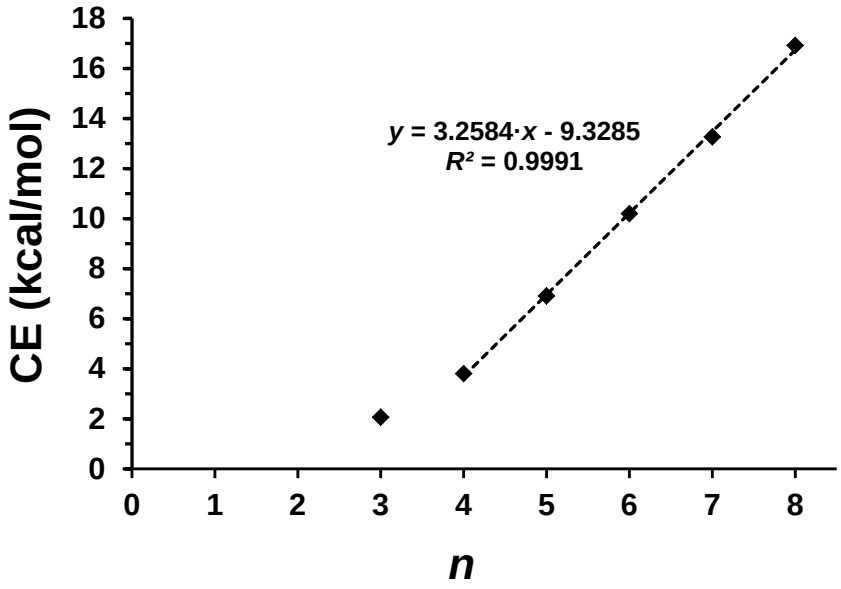


**Figure 15**

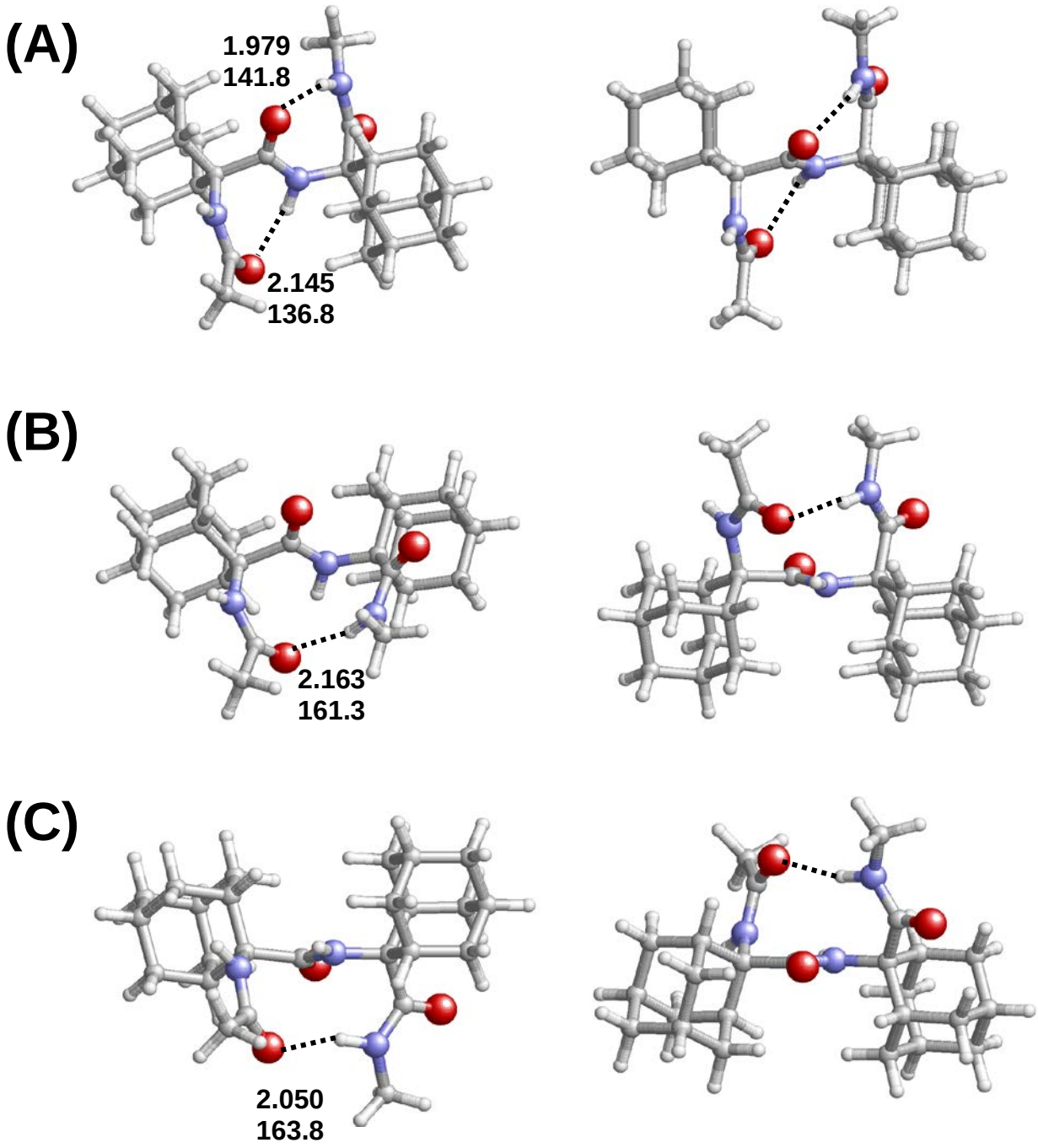


**Figure 16**